Analogue experiments on releasing and restraining bends and their application to the study of the Barents Shear Margin

Roy H. Gabrielsen–[1)], Panagiotis A. Giaennenas*[2)], Dimitrios Sokoutis[1,3)], Ernst Willingshofer[3)], Muhammad Hassaan[1,4)] & Jan Inge Faleide[1)]

[1)] Department of Geosciences, University of Oslo, Norway
[2)] Univ Rennes, CNRS, Géosciences Rennes, UMR 6118, 35000 Rennes, France
panagiotis-athanasios.giannenos@univ-rennes1.fr
[3)] Faculty of Geosciences, Utrecht University, the Netherlands
[4)] Vår Energi AS, Grundingen 3, 0250 Oslo, Norway

Corresponding author: Roy H. Gabrielsen (r.h.gabrielsen@geo.uio.no)

ORCI-id:
Jan Inge Faleide: 0000-0001-8032-2015
Roy H. Gabrielsen: 0000-0001-5427-8404
Muhammad Hassaan: 0000-0001-6004-8557

Abstract:
The Barents Shear Margin separates the Svalbard and Barents Sea from the North Atlantic. During the break-up of the North Atlantic the plate tectonic configuration was characterized by sequential dextral shear, extension, an eventuallyfinally contraction and inversion. This generated a complex zone of deformation that contains several structural families of over-lapping and reactivated structures.
A series of crustal-scale analogue experiments, utilizing a scaled stratified sand-silicon polymer sequence were utilized in the study of -the structural evolution of the shear margin.

The most significant observations of particular significance for interpretating the structural configuration of the Barents Shear Margin are:
1) Prominent early-stage positive structural elements (e.g. folds, push-ups) interacted with younger (e.g. inversion) structures and contributed to a hybrid final structural pattern.
2) Several structural features that were initiated during the early (dextral shear) stage became overprinted and obliterated in the subsequent stages.
3) All master faults, pull-part basins and extensional shear duplexes initiated during the shear stage quickly became linked in the extension stage, generating a connected basin system along the entire shear margin at the stage of maximum extension.
4) The fold pattern generated during the terminal stage (contraction/inversion became dominant in the basin areas and was characterized by fold axes striking parallel to the basin margins. These folds, however, strongly affected the shallow intra-basin layers.

The experiments reproduced the geometry and positions of the major basins and relations between structural elements (fault and fold systems) as observed along and adjacent to the Barents Shear Margin. This supports the present structural model for the shear margin.

Plain language summary:

The Barents Shear Margin defines the border between the relatively shallow Barents Sea that is situated on a continental plate, and the deep ocean. The margin is characterized by a complex structural pattern that has resulted from the opening and separation of the continent and the ocean, starting c. 65 million years ago. This history included on phase of right-lateral shear and one phase of spreading, the latter including a subphase of shortening, perhaps due to plate tectonic reorganizations. The area has been mapped by the study of reflection seismic lines for decades, but many details of its development is not yet fully constrained. We therefore ran a set of scaled experiments to investigate what kind of structures could be expected in this kind of tectonic environment, and to figure out what is a reasonable time relation between them. From these experiments we deducted several types of structures ~~,~~ (faults, folds and sedimentary basins) that help~~s~~ us to improve the understanding of the history of the opening of the North Atlantic.

Key words: Analogue experiments, dextral strike-slip, releasing and restraining bends, multiple folding, Barents Shear Margin**,** basin inversion

Introduction

Physiography, width and structural style of the Norwegian continental margin vary considerably along its strike (e.g. Faleide et al., 2008, 2015). The margin includes a southern rifted segment between 60° and 70°N and a northern sheared-rifted segment between 70° and 82°N (**Figure 1A**). The latter coincides with the ocean-ward border of the western Barents Sea and Svalbard margins (e.g. Faleide et al., 2008) and is referred to here as "the Barents Shear Margin". This segment coincides with the continent-ocean transition (COT) of the northernmost part of the North Atlantic Ocean, and its configuration is typical for that of transform margins where the structural pattern became established in an early stage of shear, later to develop into an active continent-ocean passive margin (Mascle & Blarez, 1987; Lorenzo, 1997; Seiler et al., 2010; Basile, 2015; Nemcok et al., 2016). Late Cretaceous - Palaeocene shear, rifting, breakup and incipient spreading in the North Atlantic was associated with voluminous magmatic activity, resulting in the development of the North Atlantic Volcanic Province (Saunders et al., 1997; Ganerød et al., 2010; Horni, 2017). According to its tectonic development, the Barents Shear Margin (**Figure 1B**) incorporates, or is bordered by, several distinct structural elements, some of which are associated with volcanism and halokinesis.

The multistage development combined with a complex geometry caused interference between structures (and sediment systems) in different stages of the margin development. Such relations are not always obvious, but interpretation can be supported by the help of scale-models. We c~~C~~ombin~~e~~ing the interpretation of reflection seismic data and analogue modeling~~.~~, Thus,~~therefore,~~ we investigate structures generated in (initial) dextral shear. These were generated during initial dextral shear~~,~~ the development into seafloor spreading and subsequent contraction. T~~in this process, t~~he later stages (contraction) ~~of which~~ were likely influenced by plate reorganization (Talwani & Eldholm, 1977~~;~~, Gaina et al., 2009~~;~~ see also ~~see also~~ Vågnes et al., 1998; Pascal & Gabrielsen, 2001; Pascal et al., 2005; Gac et al., 2016) or other far-field stresses (Doré & Lundin, 1996; Lundin & Doré, 1997; Doré et al., 1999; 2016; Lundin et al., 2013). The present experiments were designed to illuminate the structural complexity affiliated with multistage sheared passive margins, so that the significance of structural elements like fault and fold

systems observed along the Barents Shear Margin could be set into a dynamic context. The study area suffered

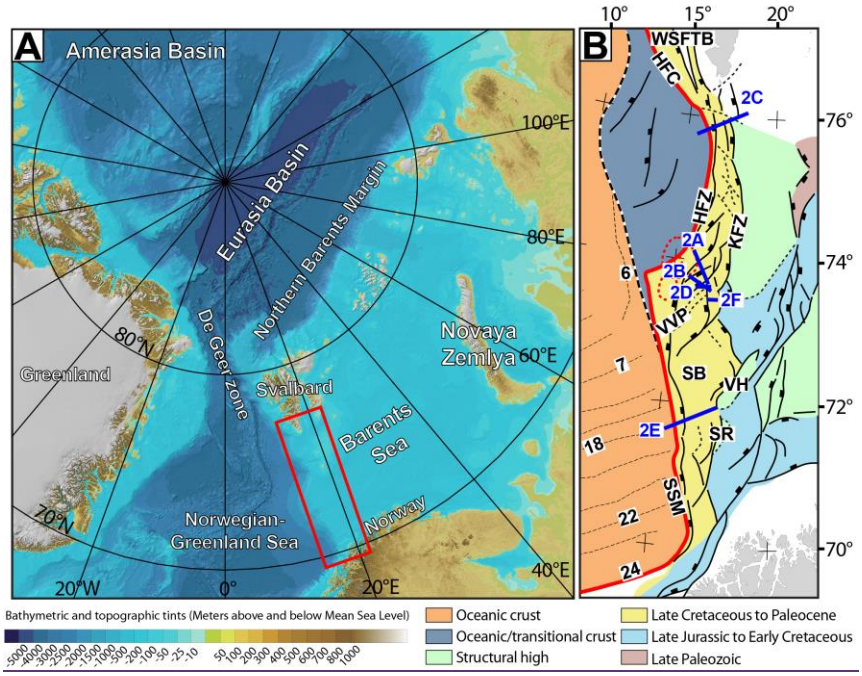

Figure 1: A) The Barents Sea is separated from the Norwegian-Greenland Sea by the de Geer transfer margin. Red box shows the present study area. **B)** Structural map Barents Sea shear margin. Note segmentation of the continent-ocean transition. Abbreviations (from north to south): WSFTB = West Spitsbergen Fold-and-Thrust Belt, HFZ = Hornsund Fault Complex, KFC = Knølegga Fault Zone, VVP = Vestbakken Volcanic Province, SB = Sørvestsnaget Basin, VH = Veslemøy High, SR = Senja Ridge, SSM = Senja Shear Margin. Blue lines indicate position of seismic profiles in Figure 2 and red line X-X´ shows western border of thinned crust (see also Figure 3). Chron numbers are indicated on oceanic crust area.

repeated and contrasting stages of deformation, including dextral shear, oblique extension, inversion and volcanic activity. This is a particular challenge in such tectonic settings, that are characterized by repeated overprinting and cannia~~b~~balization of younger structural elements. ~~—~~Results from the ~~T~~he experiments facilitate ~~al approach opens for~~ the identification and characterization of structural elements at the different stages of deformation and to identify the ~~their affiliated~~ structural elements that were developed at stages of deformation preceeding the present-day margin configuration~~geometry~~.

Regional background

In the following sections we provide definitions and a short description of the main structural elements constituting the study area. The structural elements are presented in-sequence from north to south ~~and~~ (**Figure 1B**).

The greater **Barents Shear Margin** is a part of the more extensive De Geer Zone megashear system which linked the Norwegian Greenland Sea and the Arctic Eurasia system (Eldholm et al., 1987; 2002; Faleide et al., 1988; Breivik et al., 1998; 2003). Together with its conjugate Greenland counterpart it carries the evidence of post-Caledonian extension that culminated with Cenozoic break-up of the North Atlantic (e.g. Brekke, 2000; Gabrielsen et al., 1990; Faleide et al., 1993; Gudlaugsson et al., 1998). Two shear margin segments are separated by a central rift-dominated segment along the Barents Shear Margin (Myhre et al., 1982; Vågnes, 1997; Myhre & Eldholm, 1988; Ryseth et al., 2003; Faleide at al., 1988; 1993; 2008). Each segment maintained the structural and magmatic characteristics of the crust during its development. Of these the Senja Shear Margin is the southernmost segment, originally termed the Senja Fracture Zone by Eldholm et al.~~,~~ (1987). Here NNW-SSE-striking folds interfere with NE-SW-striking structures (Giaennenas, 2018). Strain partitioning characterizes the ~~of~~the shear zone system ~~–~~(e.g. ~~V~~West Spitsbergen; Leever et al., 2011a,b and the Sørvestsnaget Basin; Kristensen et al., 2017).

The Hornsund Fault Zone and West Spitsbergen Fold-and Thrust Belt form the northernmost segment of the Barents Shear Margin. Itt~~and~~ coincides with the southern continuation of the De Geer Zone and the Senja Shear Margin. ~~The presently distinguishable master fault of this system is~~ The Hornsund Fault Zone~~,~~ belongs to this system and ~~which together with the West Spitsbergen fold-and-thrust-belt~~ provides a type setting for transpression and strain partitioning together with the West Spitsbergen fold-and-thrust-belt (Harland, 1965; 1969; 1971; Lowell, 1972; Gabrielsen et al., 1992; Maher et al., 1997; Leever et al., 2011 a,b). Plate tectonic reconstructions suggest that the plate boundary

accommodated c. 750 km along-strike dextral displacement and 20-40 km of shortening in the Eocene (Bergh et al., 1997; Gaina et al., 2009).

The Knølegga Fault Zone can be seen as a part of the Hornsund fault system extending from the southern tip of Spitsbergen (Gabrielsen et al., 1990). It trends NNE-SSW to N-S and defines the western margin of the Stappen High. The vertical displacement approaches 6 km. Although the main movements along the fault may be Tertiary of age, it is likely that it was initiated much earlier. The Tertiary displacement may have a lateral (dextral) component (Gabrielsen et al., 1990).

The Vestbakken Volcanic Province is the main topic of this contribution. It represents the central rifted segment of the ~~Senja~~Barents Shear Margin and links the sheared margin segments to the north and south occupying a right-double stepping (eastward) releasing-bend-setting. Prominent volcanoes and sill-intrusions suggest three distinct volcanic events in the Vestbakken Volcanic Province (Jebsen & Faleide, 1998; Faleide et al., 2008; Libak et al., 2012). It is constrained to its east by the eastern boundary fault (EBF in **Figure 1B**), that is a part of the Knølegga Fault Complex, separating the Vestbakken Volcanic Province from the marginal Stappen High to the east. To the south and southeast the Vestbakken Volcanic Province drops gradually towards the Sørvestsnaget Basin across the southern extension of the eastern boundary fault and its associated faults. To the west and north the area is delineated by the continent – ocean boundary/transition. The Vestbakken Volcanic Province includes both extensional and contractional structures (e.g. Jebsen & Faleide, 1998; Faleide et al., 2008; Blaich et al., 2017).

~~, and~~ Two main episodes of Cenozoic extensional faulting were identified in the Vestbakken Volcanic Province: (i) a late Paleocene-early Eocene event, which correlates in time with the continental break-up in the Norwegian-Greenland Sea, (ii) an early Oligocene event that is tentatively correlated to plate reorganization around 34 Ma activating~~ed~~ NE-SW striking faults. Volcanic activity coincides with these events.

The Sørvestsnaget Basin occupies the area east the COT between 71 and 73°N and is characterized by an exceptionally thick Cretaceous-Cenozoic sequence (Gabrielsen et al., 1990). To the west it is delineated by the Senja Shear Margin and to the northeast it is separated from the Bjørnøya Basin by the southern part of the Knølegga Fault Complex (Faleide et al., 1988). The position of the Senja Ridge coincides with southeastern border of the Sørvestsnaget Basin (Figure 1B), whereas the Vestbakken Volcanic Province is situated to its north. An episode of Cretaceous rifting in the Sørvestsnaget Basin climaxed in the Cenomanian-middle Turonian (Breivik et al., 1998), succeeded by Late Cretaceous-Palaeocene fast sedimentation (Ryseth et al., 2003). Particularly the later stages of the basin formation were strongly influenced by the opening of the North Atlantic (Hanisch, 1984; Brekke & Riis, 1987). Salt diapirism also contributed to the development of this basin (Perez-Garcia et al., 2013).

The Senja Ridge (SR in **Figure 1B**) runs parallel to the continental margin and coincides with the western border of the Tromsø Basin. It is characterized by a N-S-trending gravity anomaly which are interpreted as buried mafic-ultramafic intrusions which are associated with the Seiland Igneous Province (Fichler & Pastore, 2022). The structural development of the Senja Ridge has been associated with shear affiliated with the development of the shear margin (Riis et al., 1986). and though it was a positive structural element from the mid Cretaceous to the Pliocene it may have been activated at an even earlier stage (Gabrielsen et al., 1990).

The Senja Shear Margin was active during the Eocene opening of the Norwegian-Greenland Sea dextral shear causing ~~that~~ splitting out of slivers of continental crust. These slivers became embedded in the oceanic crust during continued seafloor spreading (Faleide et al., 2008). The Senja Shear Margin coincides with the western margin of a basin system superimposed on an area of significant crustal thinning. This part of the shear margin was characterized by a composite architecture even at the earliest stages of its development (Faleide et al., 2008). The basin system accumulated ~~-~~sedimentary sequences~~thicknesses~~ that reached thicknesses of up to 18-20 km. Subsequent shearing contributed to the

development of releasing and restraining bends, associated pull-apart-basins, neutral strike-slip segments, flower-structures and fold-systems (*sensu* Crowell, 1974 a,b; Biddle & Christie-Blick, 1985a,b; Cunningham & Mann, 2007a,b). Particularly the hanging wall west of the Knølegga Fault Complex (see below) of the Barents Shear Margin was affected by wrench deformation as seen from several push-ups and fold systems (Grogan et al., 1999; Bergh & Grogan 2003). The structural development of the margin was complicated by active halokinesis (Knutsen & Larsen, 1997; Gudlaugsson et al., 1998; Ryseth et al., 2003).

Reflection seismic data and structural interpretation

The data set of this study includes 2D seismic reflection data from several surveys and well data in the Vestbakken Volcanic Province. Data coverage is less dense in northern part of the study area. Typical spacing of seismic lines is 4 km. Well 7316/5-1 was used to correlate the seismic data with formation tops in the study area whereas published paper based correlations provided calibration and age of each seismic horizon mapped (e.g. Eidvin et al., 1993; 1998 Ryseth et al., 2003). Thr~~ee~~hree stratigraphic groups are encountered ~~present~~ in the well, namely ~~;~~ the Nordland Group (between 473 - 945 m); the Sotbakken Group (between 945-3752m) and Nygrunnen Group (between 3752-4014m) (Eidvin et al., 1993; 1998; www.npd.com). Several folds of regional significance and with axial traces that can be followed along strike for 2-3 km or more occur in the Vestbakken Volcanic Province. The folds commonly are situated in the hanging walls of extensional faults and the fold traces and the structural grain of the thick-skinned master faults are generally parallel. This shows that the position and orientation of the folds were determined by the preexisting basement structural fabric ~~affiliated with these faults~~. ~~–~~The mapping~~continuity~~ of the folds is constrained by the ~~remains obscure due to~~ spacing of refection seismic lines, so each fold trace may include undetected overlap~~–~~zones or axial off-sets. ~~that have not been detected.~~ The folds were identified on the lower Eocene, Oligocene and lower Miocene levels. All the mapped folds are either positioned in the hanging walls of extensional (sometimes inverted) master faults or are dissected by younger faults with minor throws.

Strike-slip systems and analogue shear experiments

Shear margins and strike-slip systems are structurally complex and highly dynamic, so that the eventual architecture of such systems include structural elements that were not contemporaneous (e.g. Graymer et al., 2007; Crowell, 1962; 1974a,b; Woodcock & Fischer, 1986; Mousloupoulou et al., 2007; 2008). Analogue models offer the option to study the dynamics of such relations and therefore attracted the attention of early workers in this field (e.g. Cloos, 1928; Riedel, 1929) and have continued to do so until today. Early experimental works

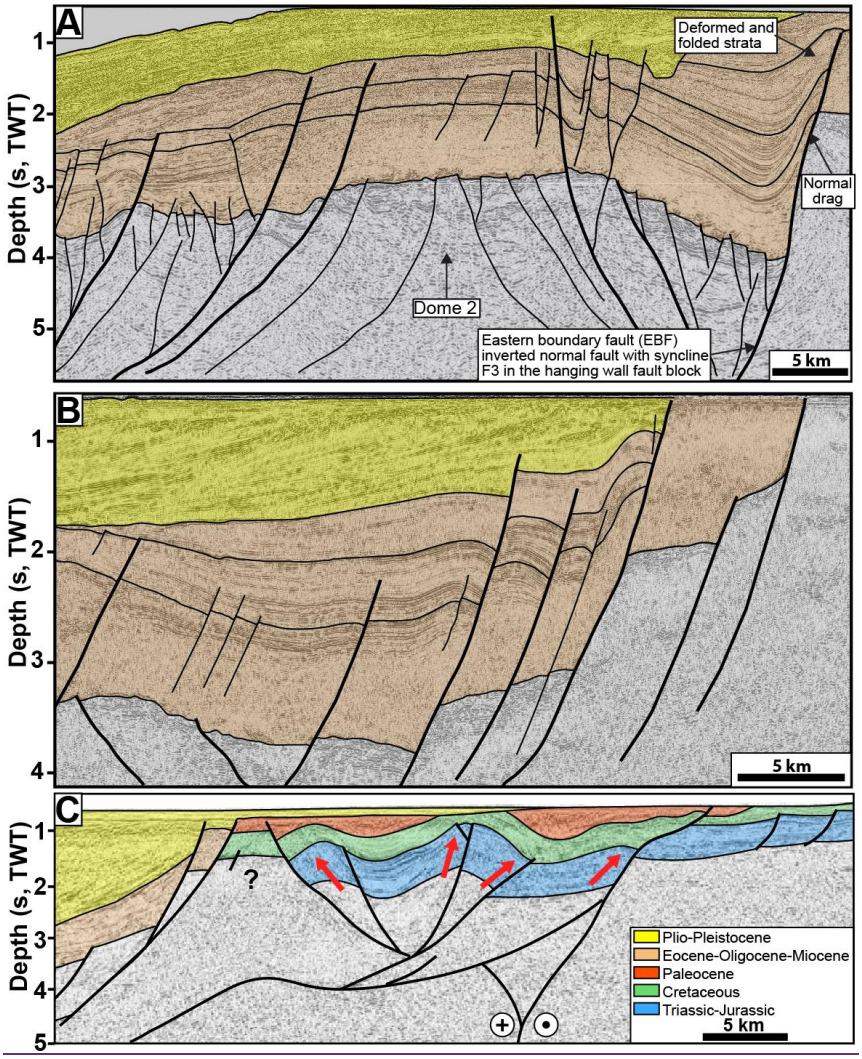

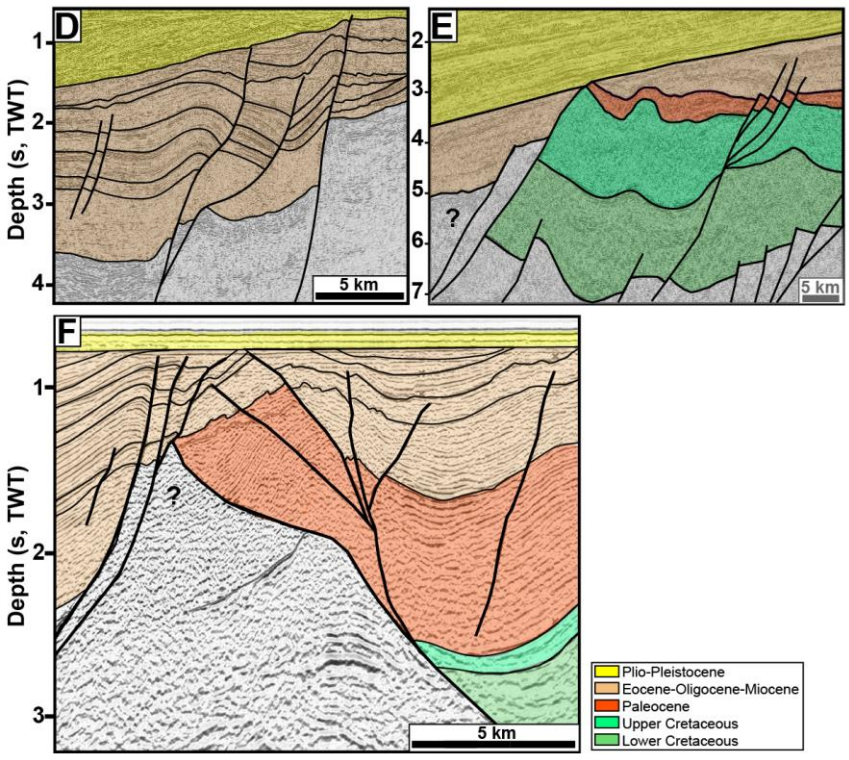

Figure 2: Seismic examples, Vestbakken Volcanic Province. **A)** Gentle, partly collapsed NE-SW-striking anticline/dome of uncertain origin in the eastern terrace domain of the southern Vestbakken Volcanic Province. **B,C**) Asymmetrical folds (fold family 2; Giannenas 2018) situated along the eastern margin of the Vestbakken Volcanic Province. These may represent primary SPE-4-structures focused in the hanging walls along margins of master fault blocks, representing reactivated SPE-2-structures. **D)** trains of symmetrical folds with upright fold axes (corresponding to PSE-5-structures) are preserved inside larger fault blocks. See text for explanation of SPE-structures. **E)** Section through push-up associated with restraining bend (PSE-4-structure). **F)** Flower (PSE-2)-structure in aera dominated by neutral shear.

mostly utilized one-layer ("Riedel-box") models (e.g. Emmons, 1969; Tchalenko, 1970; Wilcox et al., 1973), which were soon to be expanded by the study of multilayer systems (e.g. Faugère et al., 1986; Naylor et al., 1986; Richard et al., 1991; Richard & Cobbold, 1989, 1995; Schreurs, 1994, 2003; Manduit & Dauteuil, 1996; Dateuil & Mart, 1998; Schreurs & Colletta, 1998, 2003; Ueta et al., 2000; Dooley & Schreurs, 2012). The systematics and dynamics of strike-slip systems have been focused upon in a number of summaries like Sylvester (1985; 1988); Biddle & Christie-Blick (1985 a,b); Cunningham & Mann (2007); Dooley & Schreurs (2012); Nemcok et al. (2016) and Peacock et al. (2016). Concepts and nomenclature established in these works are used in the following descriptions and analysis. Also, following Christie-Blick & Biddle (1985a,b) and Dooley & Schreurs (2012) we apply the term Principal Deformation Zone (PDZ) for the junction between the movable polythene plates underlying the experiment. The contact between the fixed and movable base defined a non-stationary velocity discontinuity ("VD"; Ballard et al., 1987; Allemand & Brun, 1991; Tron & Brun, 1991).

Several experimental works have particularly focused on the geometry and development of pull-apart-basins in releasing bend settings (Mann et al., 1983; Faugére et al., 1983; Richard et al., 1995; Dooley & McClay, 1997; Basile & Brun, 1999; Sims et al., 1999; Le Calvez & Vendeville, 2002; Mann, 2007; Mitra & Paul, 2011). The pull-apart basin was described by Burchfiel & Stewart (1966) and Crowell (1974a,b) as formed at a releasing bend or at a releasing fault step-over along a strike-slip zone (Biddle & Christe-Blick, 1985a,b). This basin type has also been termed "rhomb grabens" (Freund, 1971) and "strike-slip basins" (Mann et al., 1993) and is commonly considered to be synonymous with the extensional strike-slip duplex (Woodcock & Fischer, 1986; Dooley & Schreurs, 2012). In the descriptions of our experiments, we found it convenient to distinguish between extensional strike-slip duplexes in the context of Woodcock & Fischer (1986) and Twiss & Moores, (2007, p. 140-141;) and pull-apart basins (rhomb grabens: Crowell, 1974 a,b; Aydin & Nur, 1993) since they reflect slightly different stages in the development in our experiments (see discussion).

Experimental setup

To study the kinematics of complex shear margins, a series of analogue experiments were performed at the tectonic modelling laboratory (TecLab) of Utrecht University, The Netherlands. All experiments were built on two overlapping 1 mm thick plastic sheets (each 100 cm long and 50 cm wide) that were placed on a flat, horizontal table surface. The boundary between the underlaying movable and overlaying stationary plastic sheets had the shape of the mapped continent-ocean boundary (COB; **Figure 1B**). The moveable sheet was connected to an electronic engine, which pulled the sheet at constant velocity during all three deformation stages. Displacement rates were therefore not scaled. The modelling material was then placed on these sheets where the layers on the stationary sheet represent the continental crust including the continent-ocean transition (COT) whereas those on the mobile sheet represents the oceanic crust. The model layers were confined by aluminum bars along the long sides and sand along the short sides (**Figure 3A**). The continental crust tapers off towards the oceanic crust with a relatively constant gradient. A sand-wedge with a constant dip angle determined by the difference in thickness between the intact and the stretched crust, and that covered the width of the silicon putty layer, was made to simulate the ocean-continent transition (**Figure 3B**). The taper angle was kept constant for all models.

The pre-cut shape of the plate boundary includes major releasing bends positioned so that they correspond to the geometry of the COB and the three main structural segments of the Barents Shear Margin as follows. *Segment 1* of the BarMar-experiments (**Figure 4**) contained several sub-segments with releasing and restraining bends as well as segments of "neutral" (Wilcox et al., 1973; Mann et al. 1983; Biddle & Christie-Blick, 1985b) or "pure" (Richard et al., 1991) strike-slip. *Segment 2* had a basic crescent shape, thereby defining a releasing bend at its southern margin in the position similar to that of the Vestbakken Volcanic Province, that merged into a neutral shear-segment along the strike of, whereas a restraining bend occupied the northern margin of the segment. *Segment 3* was a straight basement segment, defining a zone of neutral shear and corresponds to the strike-slip segment west of Svalbard (**Figure 1**).

The experiments included three stages of deformation with constant rates of movement of the mobile sheet at 10 $cmhr^{-1}$ in all three stages. The relative

angles of plate movements in the experiments were taken from post late Paleocene opening directions in the northeast Atlantic (Gaina et al., 2009). Dextral shear was applied in the *first phase* in all experiments by pulling the lower plastic sheet by 5 cm. In the *second phase* the left side of the experiment was extended by 3 cm orthogonally (BarMar6) or obliquely (315 degrees; BarMar 8 & 9) to the trend of the shear margin, whereas plate motion was reversed during the *third phase of deformation*, leading to inversion of earlier formed basins that had been

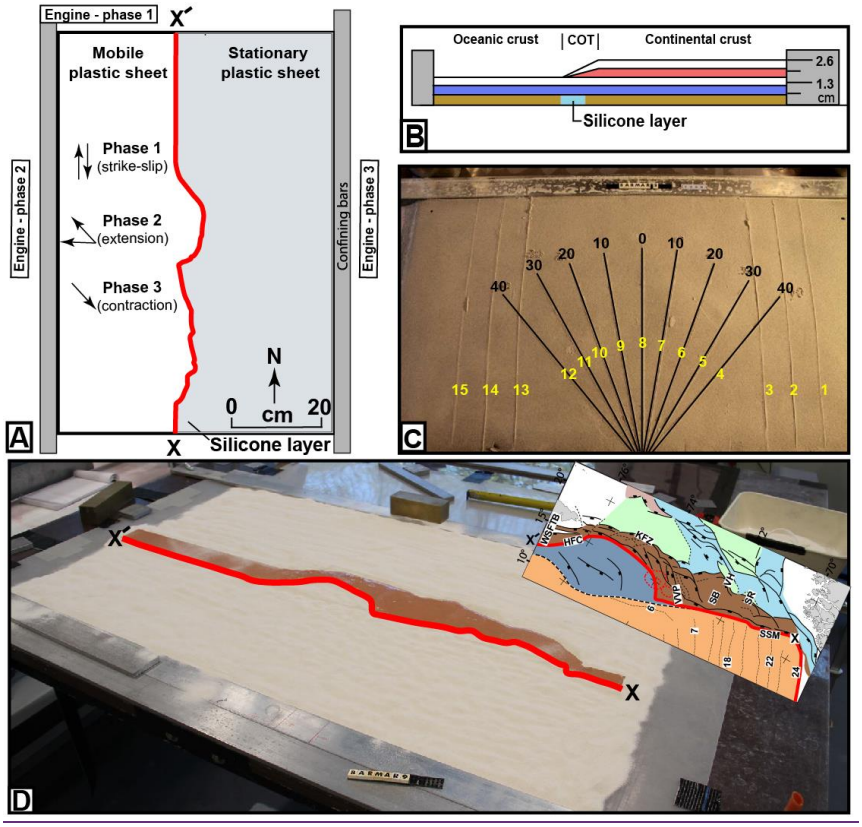

Figure 3: A) Schematical set-up of BarMar3-experiment as seen in map view. **B)** Section through same experiment before deformation, indicating stratification and thickness relations. **C)** Standard positions and orientation for sections cut in all experiments in the BarMar-series. Yellow numbers are section numbers. Black numbers indicate angle between the margins of the experiment (relative to N-S) for each profile. **D)** Outline of silicone putty layer as applied in all experiments. Inset shows original structural map of the Barents Margin used to define the width of the thinned crust. Red line (X-X') indicates the western limit of the thinned zone.

developed in the strike-slip and extensional phases. Sedimentary basins that develop due to strike-slip (phase 1) or extension (phase 2) have been filled with layers of colored feldspar sand by sieving, so that a smooth surface was obtained. These layers are primarily important for discriminating among deformation phases and thus act as marker horizons. Phase 3 was initiated by inverting the orthogonal (BarMar6) or oblique (BarMar 8 & 9) extension of Phase 2 to contraction as a proxy for ridge-push that likely was initiated when the mid-

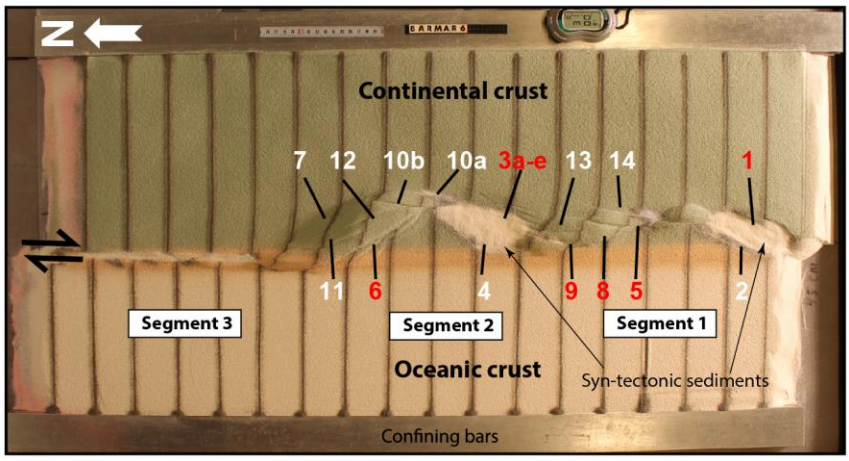

Figure 4: Position of segments and major structural elements as referred to in the text and subsequent figures (see particularly **Figures 5 and 6**). This example is taken from the reference experiment BarMar6. All experiments BarMar6-9 followed the same pattern, and the same nomenclature was used in the description of all experiments and provides the template for the definition of structural elements in **Figure 7**.

oceanic ridge was established in Miocene time in the North Atlantic (Moser et al., 2002; Gaina et al., 2009). Contraction generated by ridge-push has been inferred from the mid Norwegian contin~~u~~ental shelf (Vågnes et al., 1998; Pascal & Gabrielsen, 2001; Faleide et al., 2008; Gac et al., 2016) and seems still to prevail in the northern areas of Scandinavia (Pascal et al., 2005), although far-field compression generated by other processes have been suggested (e.g. Doré & Lundin, 1996).

Coloured layers of dry feldspar sand represent the brittle oceanic and continental crust. This material has proven suitable for simulating brittle

deformation conditions (Willingshofer et al., 2005; Luth et al., 2010; Auzemery et al., 2021). It~~and~~ is characterized by a grain size of 100-200 µm, a density of 1300 kgm^{-3}, a cohesion of ~16-45 Pa and a peak friction coefficient of 0.67 (Willingshofer et al., 2018). Additionally, a 8 mm thick and of variable width corresponding to the transition zone (as mapped in reflection seismic data) of 'Rhodorsil Gomme GSIR' (Sokoutis, 1987) silicone putty mixed with fillers was used as a proxy for the thinned and weakened continental crust at the ocean-continent transition (**Figure 1B and 3A,B**). This Newtonian material (n=1.09) has a density of 1330 $kgm^{-3}$and a viscosity of $1.42x10^4$ Pa.s.

The experiments were scaled following standard scaling procedures as described by Hubbert (1937), Ramberg (1967) or Weijermars and Schmeling (1986), assuming that inertia forces are negligible when modelling tectonic processes on geologic timescales (see Ramberg (1981) and Del Ventisette et al. (2007) for a discussion on this topic). The models were scaled so that 10 mm in the model approximates c. 10 km in nature yielding a length scale ratio of $1.00E^{-6}$. As such, the model oceanic and continental crusts scale to 18 and 26 km in nature, respectively, which, although slightly overestimating the ~~most intensely thinned~~ oceanic crustal thickness (10-12 km) is in full agreement with the estimated thickness of the thinned oceanward segment of the continental crust (30-20 km Breivik et al., 1998).

The brittle crust, dry feldspar sand, deforms according to the Mohr-Coulomb fracture criterion (Horsfield, 1977; Mandl et al., 1977; McClay, 1990; Richard et al., 1991; Klinkmüller et al., 2016), whereas silicone putty promotes ductile deformation and folding. The geometry applied in the present experiments is accordingly well suited for the study of the COB in the Barents Shear Margin (Breivik et al., 1998).

When complete, the experiments were covered with a thin layer of sand further to stabilize the surface topography before the models were saturated with water and cross-sections that were oriented transverse to the velocity discontinuity were cut in a fan-shaped pattern (**Figure 3C**). All experiments have been monitored with a digital camera providing top-view images at regular time intervals of one minute.

All experiments performed were oriented in a N-S-coordinate framework to facilitate comparison with the western Barents Sea area and had a three-stage deformation sequence (dextral shear – extension – contraction). All descriptions and figures relate to this orientation. It was noted that all experiments reproduced comparable basic geometries and structural types, demonstrating robustness against variations in contrasting strength of the "ocean-continent"-transition zone, which included ~~by~~ a zone of silicone putty with variable width below an eastward thickening sand-wedge (**Figure 3B**). ~~and changing displacement velocities.~~ The experiments were terminated before the full closure of the basin system, in accordance with the extension vector > contraction vector as in the North Atlantic (see Vågnes et al. 1998; Pascal & Gabrielsen 2001; Gaina et al. 2009).

Modelling Results

A series of nine experiments (BarMar1-9) with the set-up described above was performed. Experiments BarMar1-5 were used to calibrate and optimize geometrical outline, deformation rate, and angles of relative plate movements and are not shown here. The optimized geometries and experimental conditions were utilized for experiments BarMar6-9, of which BarMar6 and 8 (and some examples from BarMar9) ~~and~~ are illustrated here. ~~,~~ They yielded similar results in that all crucial structural elements (faults and folds) were reproduced in all experiments as described in the text are shown in **Figure 4**. ~~)~~ It is emphasized that the extensional basins affiliated with the extension phase (phase 2) were ~~became~~ wider for ~~in~~ the orthogonal (BarMar6) as compared to the oblique extension experiments (BarMar 8) (**Figures 5 and 6**). Furthermore, the fold systems generated in the experiments that utilized oblique contraction of 3145/135^0 (BarMar8-9) produced more extensive systems of non-cylindrical folds. These folds also had ~~with~~ continuous, but more curved fold traces as compared to the experiments with orthogonal extension/contraction (BarMar6). The fold axes generally rotated to become parallel to the (extensional) master faults delineating the pull-apart basins generated in deformation stage 1 in experiments with an oblique opening/closing angle.

Examples of the sequential development is displayed in **Figures 5 and 6**, and summarized in **Figure 7**. Elongated positive structural elements with fold-like morphology as seen on the surface were detected during the various stages of the present experiments. The true nature of those were not easily determined until the experiments were terminated and transects could be examined. Such structures included buried push-ups (*sensu* Dooley & Schreurs, 2012), antiformal stacks, back-thrusts, positive flower structures, fold trains, and simple anticlines. For convenience, we use the non-genetic term "positive structural elements" termed *PSEm-n* for such structure types as seen in the experiments in the following description. In the following the deformation in each segment is characterized for the three deformation phases **(Table 1).**

Table 1

Characteristics of Positive Structural Element (PSE 1-6) as described in the text and shown in figures. Note that the PSE-1-structures that were developed in the earliest stages of the experiments became cannibalized during the continued deformation. No candidates of these structures were identified in the reflection seismic sections.

Struct. type	Structural configuration	Orientation	Expr. stage	Segment	Recognized in seismic	Figure Expr	Figure Seism
PSE-1	Open syn-anticline system	135 deg	Stage 1	1,3	?	5,6	1A?
PSE-2	Incipient flower or half-flower	Parallel master fault	Stage 1	1,2,3	Yes	5,6,8	1B
PSE-3	Forced folds above rotated fault blocks	Parallel master fault in releasing bend	Stage 2	1,2	Yes	9B	
PSE-4	Push-up	Paralllel master fault in restraing bend	Stage 1	2	Yes	9D	1C
PSE-5	Anticlines/snake-heads in hanging walls	Parallel master faults	Stage 3	1,2,3	Yes	9C,D	1D,E
PSE-6	Anticline-syncline trains	Parallel master faults	Stage 3	1,2,3	Yes	12	1F

Formatted: Left: 2,54 cm, Right: 2,54 cm, Top: 3,17 cm, Bottom: 3,17 cm, Width: 29,7 cm, Height: 20,99 cm

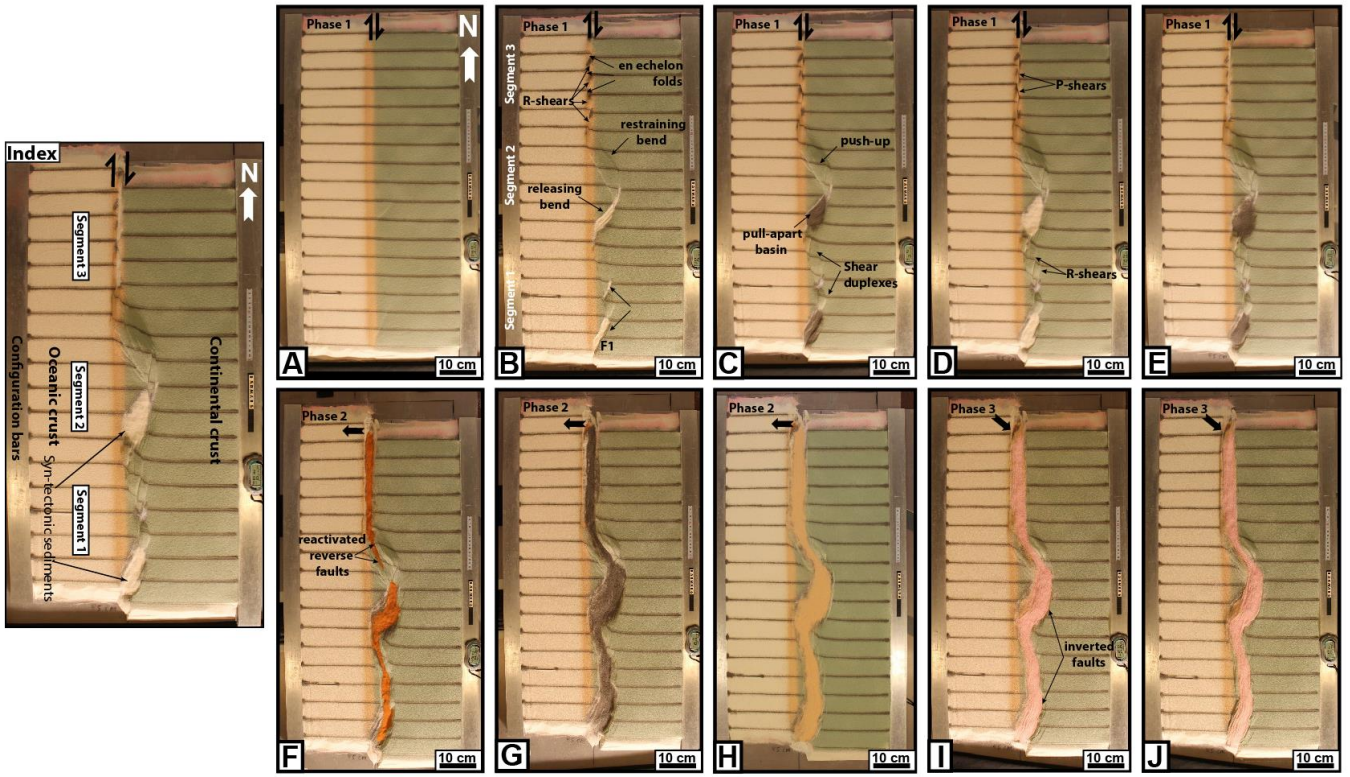
Index
N
Segment 3
Segment 2
Segment 1
Oceanic crust
Continental crust
Syn-tectonic sediments
Configuration bars
Phase 1
Phase 2
Phase 3
A
B
C
D
E
F
G
H
I
J
10 cm
en echelon folds
R-shears
restraining bend
releasing bend
F1
push-up
pull-apart basin
Shear duplexes
P-shears
R-shears
reactivated reverse faults
inverted faults

482

Figure 5: Sequential development of experiment BarMar6 by 0.5, 2.4, 3.5, 4.0 and 5.0 cm of dextral shear (Steps A-E), orthogonal extension (steps F-H) and oblique contraction (steps I-J). The master fault strands are numbered in **Figure 4**, and the sequential development for each structural family is shown in **Figure 7**. The reference panel to the upper left shows the positions of the segments.

Formatted: Indent: First line: 0 cm

Deformation phase 1: Dextral shear stage

Segment 1: Differences in the geometry of the pre-cut fault trace between segments 1, 2 and 3 became visible ~~became evident~~ after the very initial deformation stage. Particularly in segments 1 and 3 an array of oblique *en échelon* folds in between Riedel shear structures (*PSE-1-structures*) oriented c. 135º(NW-SE) to the regional VD rotating towards NNW-SSE by continued shear (**Figure 8**; see also Wilcox et al., 1973; Ordonne & Vialon, 1983; Richard et al., 1991; Dooley & Schreurs, 2012). These were simple, harmonic folds with upright axial planes and fold axial traces extending a few cm beyond the surface shear-zone described above. They had amplitudes on the scale of a few millimeters and wavelengths on scale of 5 cm. The PSE-1-structures interfered with or were dismembered by younger structures (Y-shears and PSE-2-structures; see below) causing northerly rotation of individual intra-fault zone lamellae (remnant PSE-1-structures; **Figure 8**). Structures similar to PSE-1-fold arrays are known from almost all strike-slip experiments reported and described in the literature ~~from the early works~~ (e.g. Cloos, 1928; Riedel, 1929~~.~~; See Dooley & Schreurs, 2012 for summary) and are therefore not given further attention here.

By 0.25 cm of horizontal displacement in segment 1, which included releasing and restraining bends separated by a central strand of neutral shear, a slightly curvilinear surface trace of a NE-SW-striking, top-NW normal fault in the southernmost part of segment 1 developed. This co-existed with the PSE-1-structures and became paralleled by a normal fault with opposite dip (fault 2, **Figure 4**) so that the two faults constrained a crescent- or spindle-shaped incipient extensional shear duplex (**Figures 5B and 6B**; see also Mann et al., 1983; ~~Christie-Blick & Biddle, 1985; Mann 2007; Dooley & Schreurs, 2012~~).

A system of ~~*en échelon*~~ separate *en échelon* N-S to NNE-SSE-striking normal and shear fault segments ~~that~~ became visible in segment 1 after ca. 1 cm of shear (**Figure 5C,D**). These faults did not have the orientations as expected for R (Riedel) - and R' (anti-Riedel)- shears (that would be oriented with angles of approximately 15 and 75º from the master fault trace) but became progressively

519 linked with along strike growth and the development of new faults and fault
520 segments. They thereby acquired the characteristics of Y-shears (oriented sub-
521 parallel to the master fault trace), dissecting the PSE-1-structures. By 2.4 cm of
522 shear, segment 1 had become one unified fault array (**Figures 5D and 6D**),
523 delineating a system of incipient

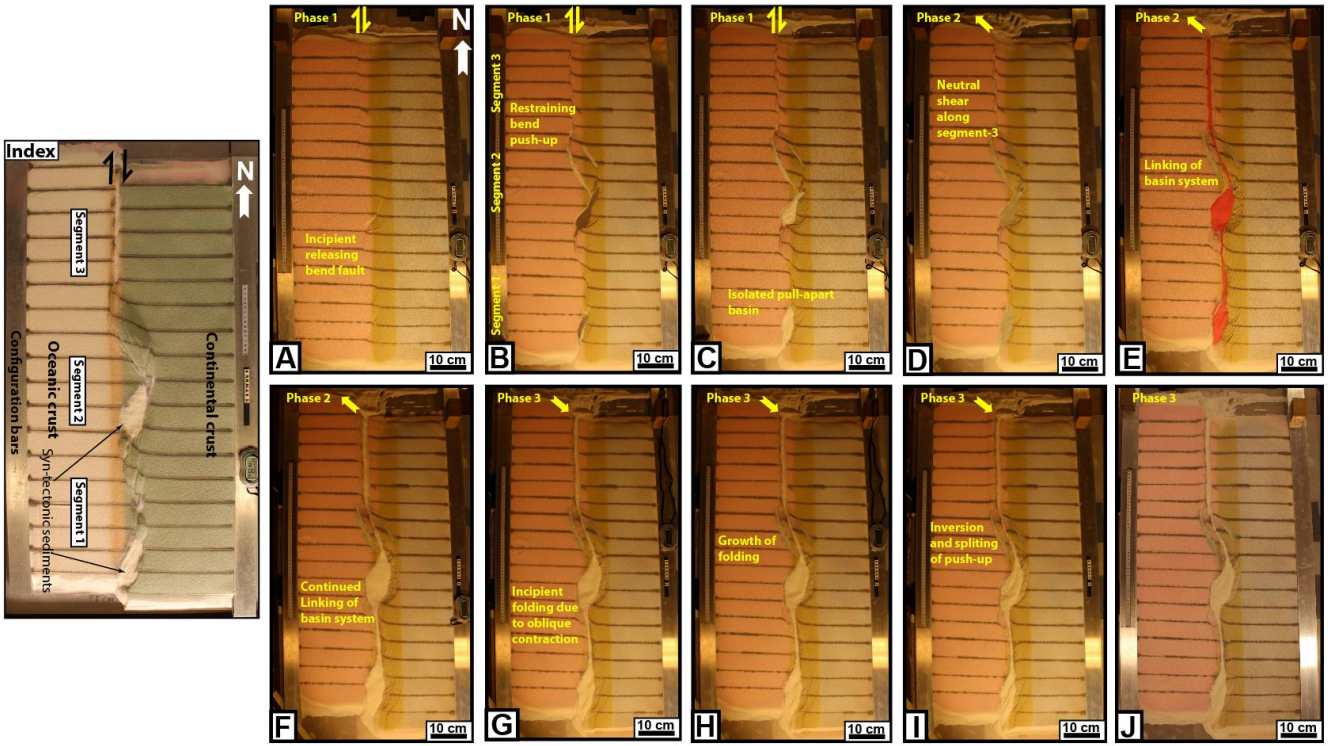

524

525 **Figure 6:** Sequential development of experiment BarMar8 by 0.5, 2.4, 3.5, 4.0 and 5.0 cm of dextral shear (Steps A-E), oblique extension
526 (steps F-H) and oblique contraction (steps I-J). The master fault strands are numbered in **Figure 3**, and the sequential development for

Formatted: Left: 2,54 cm, Right: 2,54 cm, Top: 3,17 cm, Bottom: 3,17 cm, Width: 29,7 cm, Height: 20,99 cm

Formatted: Indent: First line: 0 cm, Line spacing: single

each structural family is shown in **Figure 7**. Phases 2 and 3 involved oblique (315^0) extension and contraction in this experiment. The reference panel to the upper left shows the positions of the segments.

push-ups or positive flower structures (*PSE-2-structures;* **Figures 8 and ~~Figure~~ 10, sections B1 and B3**).

The PSE-2-structures had amplitudes of 1 - 2 cm and wavelengths of 3 - 5 cm as measured on the surface with fault surfaces that steepened down-section, the deepest parts of the structures having cores of sand-layers deformed by open to tight folds. The folds had upright or slightly inclined axial planes, dipping up to 55°, mainly to the east. The structures also affected the shallowest layers down to 1-2 cm in the sequence, but the shallowest sequences were developed at a later stage of deformation and were characterized by simple gentle to open anticlines. These structures were constrained to a deformation zone directly above the trace of the basement fault, similar to that commonly seen along shear zones (e.g. Tchalenko, 1971; Crowell, 1974 a,b; Dooley & Schreurs, 2012). This zone was 3-4 cm wide and remained stable throughout deformation stage 1 and was restricted to the close vicinity of the basement shear fault itself. A horse-tail-like fault array developed by ca. 3 cm of shear at the transitions between segments 1 and 2 (**Figures 5B-D and 6B-D)**.

The structuring in *Segment 2~~;~~* was ruled by the pre-cut crescent-shaped basement fault (velocity discontinuity) that caused the development of ~~—~~a releasing bend along its southern, and a restraining bend along its northern border (**Figure 11**). The first fault of fault array 3a-e in the southern part of Segment 2 (**Figure ~~–~~4**) was activated after c. 0.15 cm of bulk horizontal displacement (**Figure 7**). It was situated directly above the southernmost precut releasing bend, defining the margin of crescent-shaped incipient extensional strike-slip duplexes (in the context of Woodcock & Fischer, 1986, Woodcock & Schubert, 1994 and Twiss & Moores, 2007, p. 140-141). The developing basin got a spindle-shaped structure and developed into a basin with a lazy-S-shape (Cunningham & Mann, 2007; Mann, 2007). The basin widened towards the east by stepwise footwall collapse, generating sequentially rotating crescent-shaped extensional fault blocks that became trapped as extensional horses in the footwall of the releasing bend (**Figure 11**). In the areas of the most pronounced extension the crestal part of the rotational fault blocks became elevated above the basin floor, generating ridges that influenced the basin floor topography and hence, the

Formatted: Indent: First line: 0 cm

sedimentation. By continued rotation of the fault blocks and simultaneous sieving of sand the crests

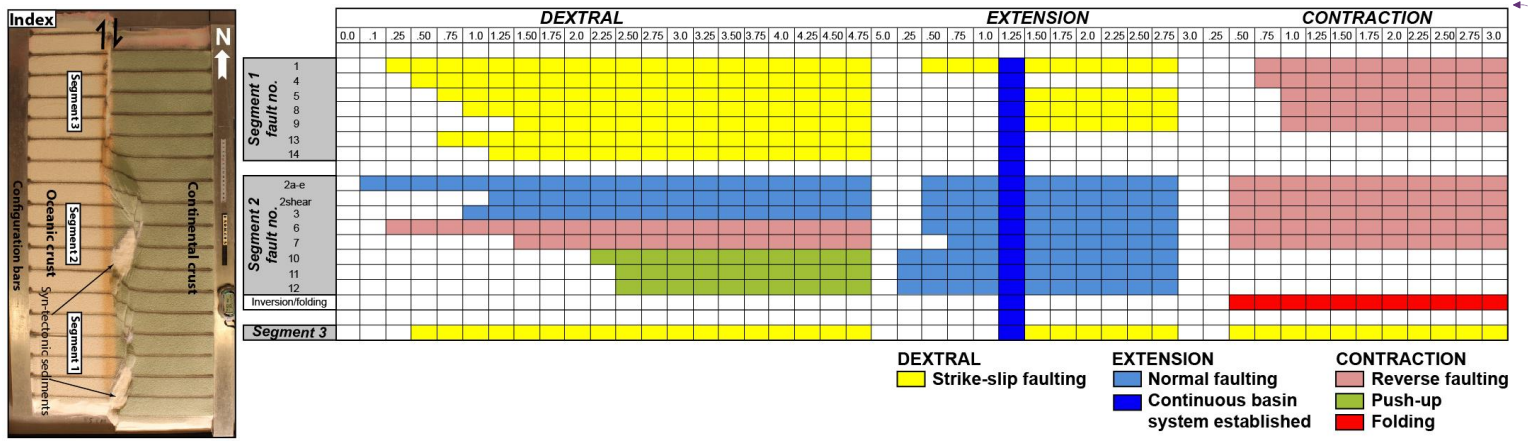

Figure 7: Summary of sequential activity in each master fault in Experiment BarMar6 (**Figure 5**) (for position of each fault, see **Figure 4**). Type and amount of displacement is shown in two upper horizontal rows. The vertical blue bar indicates the stage at which full along-strike communication became established between marginal basins. Color code (see in-set) indicates type of displacement at any stage. The reference panel to the left shows the positions of the segments.

Formatted: Left: 2,54 cm, Right: 2,54 cm, Top: 3,17 cm, Bottom: 3,17 cm, Width: 29,7 cm, Height: 20,99 cm

of the blocks became sequentially uplifted, generating forced folds (Hamblin, 1965; Stearns, 1978; Groshong, 1989; Khalil & McClay, 2016) (**Figure 10A**). In the analysis we used the term *PSE-3-structures* for these features. Simultaneously, an expanding sand-sequence became trapped in the footwalls of the master faults, defining typical growth-fault geometries.

By a shear displacement of 0.55 cm additional curved splay faults were initiated from the northern tip of the master fault of fault 3f; **Figure 7**), delineating the northern margin of a rhombohedral pull-apart-basin (Mann et al., 1983; Mann, 2007; Christie-Blick & Biddle, 1985) and with a geometry that was indistinguishable from pull-apart basins or rhomb grabens affiliated with unbridged *en échelon* fault arrays (Crowell, 1974 a,b; Aydin & Nur, 1993). Although sand was filled into the subsiding basins to minimize the graben relief

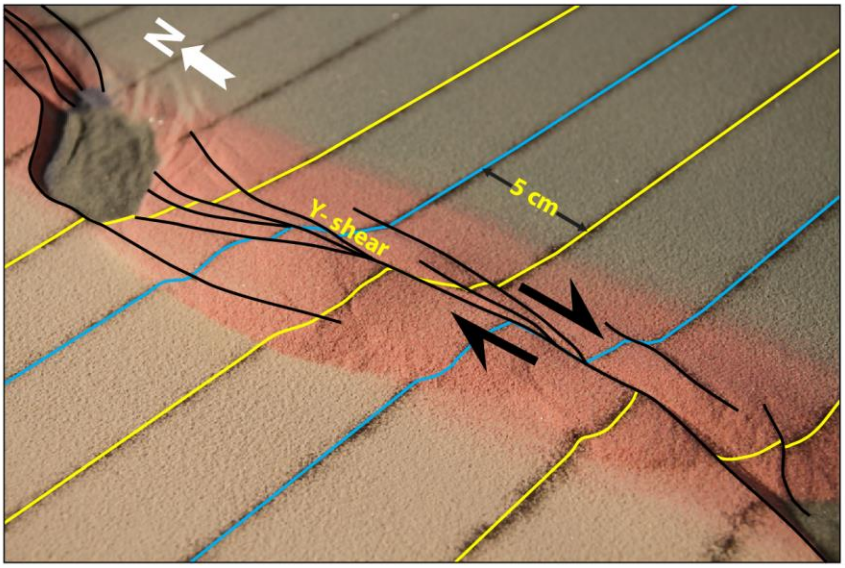

Figure 8: PSE-1 anticline-syncline pairs in segment 1 of experiment BarMar6 in an oblique view (see **Figure 4** for position of Segment 1). PSE-1 folds (indicated by relief defined by blue and yellow markers) were constrained to the central fault zone (defined by Y-shear and its splay faults) and extended only 3-4 cm beyond it. PSE-2 structures (incipient push-ups and positive flower structures) were delineated by shear faults (black lines) and completely cannibalized PSE-1 structures by continued shear. Yellow and blue reference lines illustrate the rotation of the fold axial trace caused by dextral shear. Already pre-shear distance between the markers (blue and yellow lines) was 5cm. Black arrow indicates shear direction.

Formatted: Indent: First line: 0 cm

and to prevent gravitational collapse, the sub-basins that were initiated in the shear-stage were affected by internal cross-faults, and the initial basin units remained the deepest so that the buried internal basin topography maintained a high relief with several apparent depo-centers separated by intra-basinal platforms.

Systems of linked shear faults and PSE-structures became established in the central part with neutral shear that separate the releasing and restraining bends and development similarly to that seen for segment 3 (see below), but these structures were soon destroyed by the ~~combined~~ interaction between ~~development of~~ the northern and southern tips of the extensional and contractional shear duplexes (**Figure 10**).

The first structure to develop in the regime of the restraining bend (segment 2; was a top-to-the-southwest (antithetic) thrust fault at an angle of 145^0 with the regional trend of the basement border as defined by segments 1 and 3 (Fault 6). It became visible by 0.5 cm of displacement. The northern part of segment 2 became, however, dominated by a synthetic contractional top-to-the-northeast fault that was initiated by 0.85 cm of shear (Fault 7; **Figures 5 and 6**). Thus, faults 6 and 7 delineated a growing half-crescent-shaped 5-7-cm wide push-up structure (Aydin & Nur, 1982; Mann et al., 1983) south of the restraining bend (**Figure 9**; *PSE-4-structures*). By continued shear these structures got the character of an antiformal stack.

Segment 3 defined a straight strand of neutral shear. Its development in the BarMar-experiments followed strictly that known from numerous published experiments (e.g. Tchalenko, 1970; Wilcox et al., 1973; Harding, 1974; Harding & Lowell, 1979; Naylor et al., 1986; Sylvester, 1988; Richard et al., 1991; Woodcock & Schubert, 1994; Dauteuil & Mart, 1998; Mann, 2007; Casas et al., 2001; Dooley & Schreurs, 2012). A train of Riedel-shears, occupying the full length of the segment, appeared simultaneously on the surface after a shear displacement of 0.5 cm, occupying a restricted zone with a width of 2-3 cm. The Riedel-shears dominated the continued structural development of Segment 3. Riedel'-shears were absent throughout the experiments, as should be expected for a sand-dominated sequence (Dooley & Schreurs, 2012). P-shears developed by continued

shear, creating linked rhombic structures delineated by the Riedel- and P-shears generating positive structural elements with NW-SE- and NNE-SSE-striking axes

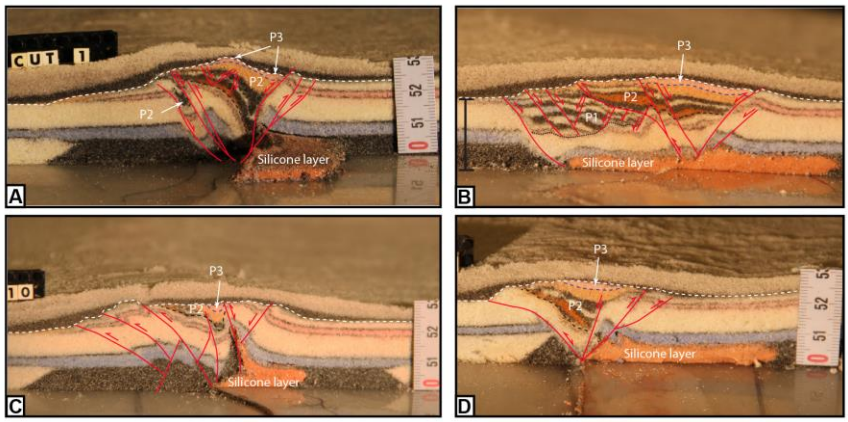

Figure 9: Cross-sections through PSE-2-related structures. PSE-structures are marked with P and PSE-number as described in text (see also Table 1). **A)** Folded core of incipient push-up/positive flower structure in segment 1, experiment BarMar6. The fold structure is completely enveloped of shear faults that have a twisted along-strike geometry. Note that the eastern margin of the structure developed into a negative structure at a late stage in the development (filled by black-pink sand sequence) and that the silicone putty sequence (basal pink sequence) was entirely isolated in the footwall. **B)** Similar structure type in experiment BarMar8. However, the basal silicone putty layer here bridged the basal high-strain zone so that folding occurred in the footwall as well as in the hanging. Folds propagated up-section into the sand layers (blue). The folds in upper (pink) layers are younger and were associated with the contractional stage (PSE-6-structures). **C)** Contraction associated with "crocodile structure" in the footwall of the main fault in segment 1, experiment BarMar8. Note disharmonic folding with contrasting fold geometries in hanging wall and footwall and at different stratigraphic levels in the footwall, indicating that shifting stress situation in time and space occurred in the experiment. **D)** Transitional fault strand between to more strongly sheared fault segments (experiment BarMar9).

(see also Morgenstern & Tchalenko, 1967), soon coalescing to form Y-shears. Transverse sections document that these structures were cored by push-up anticlines, positive half-flower structures and full-fledged positive flower structures in the advanced stages of shear (*PSE-4-structures*) (**Figures 5 and 6**; **See also Figure 10**). These were accompanied by the development of *en échelon* folds and flower structures as commonly reported from strike-slip faults in nature and in experiments. The width of the zone above the basal fault remained almost constant throughout the experiments, but was somewhat wider in experiments

with thicker basal silicone polymer layers, similar to that commonly described from comparable experiments (e.g. Richard et al., 1991).

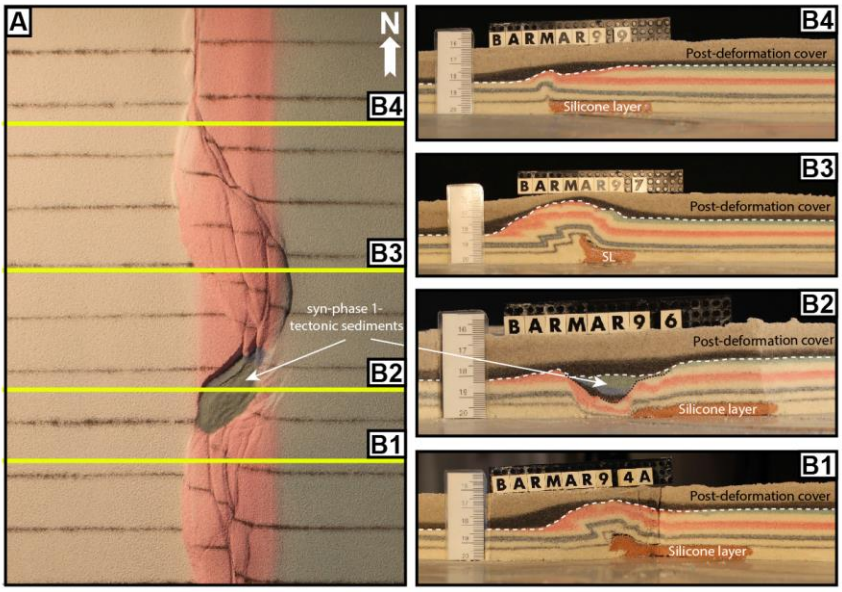

Figure 10: A) contrasting structural styles along the master fault system in segment 2 in map view and **(B)** cross sections of experiment BarMar9. SL denotes silicone layer, the stippled line the boundary between pre-and syn-deformation layers and the white dashed line the boundary with the post-deformation layers.

Deformation Phase 2: Extension

The late Cretaceous-Palaeocene dextral shear was followed by pure extension that accompanied~~ing~~ the opening along the Barents Shear Margin in the Oligocene. Our experiments focused on the effects of oblique extension, acknowledging that plate tectonic reconstructions of the North Atlantic suggest an extension angle of 315° (Gaina et al., 2009).

All strike-slip basins widened in the extensional stage~~,~~ and as one would expect, the basins generated in orthogonal extension became wider than those generated in oblique extension. In both cases, however, extension promoted enhanced ~~the~~ relief that had been generated in the shear-stage. In the earliest extensional stage, the strike-slip basin in segment 2 dominated the basin configuration~~, but b~~By continued extension the linear segments and the minor pull-apart basins in segments 1 and 2 started to open and ~~to~~ became interlinked,

subsequently generating a linked basin system that runs parallel to the entire shear margin (**Figures 5F-G, 6F-G**). The basins had become completely interlinked by an extension of 1.25 cm (marked by the vertical dark blue line in **Figure 7**). The orthogonal extension-phase also reactivated and linked several master faults that were established in deformation phase 1 (**Figures 5A and 6A**). This became evident by an extension of 0,25 – 0,50 cm and included the southern fault margin, the push-up and the splay faults defining the crestal collapse graben (Faults 6, 11 and 12; **Figure 4**). Among the faults that remained inactive throughout the extension phase were the antithetic contractional fault delineating the push-ups in segment 2 (Fault 6; **Figure 4**). The Y-shear in Segment 3 was reactivated as a straight, continuous extensional fault in phase 2. Total extension in stage 2 was 5 cm.

Deformation Phase 3: contraction

In our experiments the extension stage was followed by oblique contraction (parallel to the direction of extension as applied for each experiment). A part of the early-stage contraction was accommodated along new faults. It was more common, however, that faults that had been generated in the strike-slip and extensional stages became reactivated and rotated, and the development of isolated folds, which were commonly associated with inverted fault traces, generating snake-head or harpoon-structures structures (Cooper et al., 1989; Coward, 1994; Allmendinger, 1998; Yameda & McClay, 2004; Pace & Calamitra, 2014); *PSE-5-stuctures*). The dominant structures affiliated with the contractional stage was still new folds with traces oriented orthogonal to the shortening direction and sub-parallel to the preexisting master fault systems that defined the margin and basin margins (**Figure 12**). Also, some deep fold sets that had been generated during the strike-slip phase and seen as domal surface features became reactivated, causing renewed growth of surface structures (see **Figure 10** and explanation in figure caption). These folds were generally up-right cylindrical buckle folds in the initial contractional and with very large trace length: amplitude-ratio (*SPE-6-structures*). Some intra-basin folds, however, defined fold arrays that diagonally crossed the basins in a diagonal fashion. Particularly the folds situated along the basin margins developed into fault propagation-folds

above low-angle thrust planes. Such faults aligning the western basin margins could have an antithetic attitude relative to the direction of contraction.

During the contractional phase the margin-parallel, linked basin system started immediately to narrow and several fault strands became inverted. The basin-closure was a continuous process until the end of the experiment by 3 cm of contraction. The contraction was initiated as a proxy for an ESE-directed ridge-push stage. The first effect of this deformation stage was heralded by uplift of the margin of the established shear zone that ~~that~~ had developed into a rift during deformation stage 2. This was followed by the reactivation and inversion of some master faults (e.g. fault a2; ~~eg.~~ **Figure 4**) and thereafter by the development of a new set of low-angle top-to-the-ESE contractional faults. These faults displayed a sequential development~~,~~ (fault family 1; **Figure 7**) and were associated with folding of the strata in the rift structure, probably reflecting foreland-directed in-sequence thrusting (SPE-5 and PSE-6 fold populations).

Discussion

The break-up and subsequent opening of the Norwegian-Greenland Sea was a multi-stage event (**Figure 13**) that imposed shifting stress configurations overprinting the already geometrically complex Barents Shear Margin. Therefore, scaled experiments were designed to illuminate its structural development. The experiments utilized three main segments that correspond to the Senja Fracture Zone (segment 1), the Vestbakken Volcanic Province (segment 2) and the Hornsund Fault Zone (segment 3) respectively and three deformation phases (dextral shear, oblique ~~co~~extension and contraction). Several structural families (PSE 1-6) generated in the experiments correspond to structural features observed in reflection seismic sections. In the following discussion we utilize these two data sets in explaining the sequential development of each segment of the shear margin.

Structures of phase 1 (dextral shear)

Segment 1 ~~in the experiments~~ (~~which~~ corresponding~~s~~ to the Senja Fracture Zone) was dominated by neutral dextral shear, although jogs in the (pre-cut) fault provided minor sub-segments with subordinate releasing and restraining bends.

PSE-1-folds seen i~~o~~n the incipient shear phase ~~-~~were confined to the area just above the basal master fault (VD) and its immediate vicinity (see also experiments in

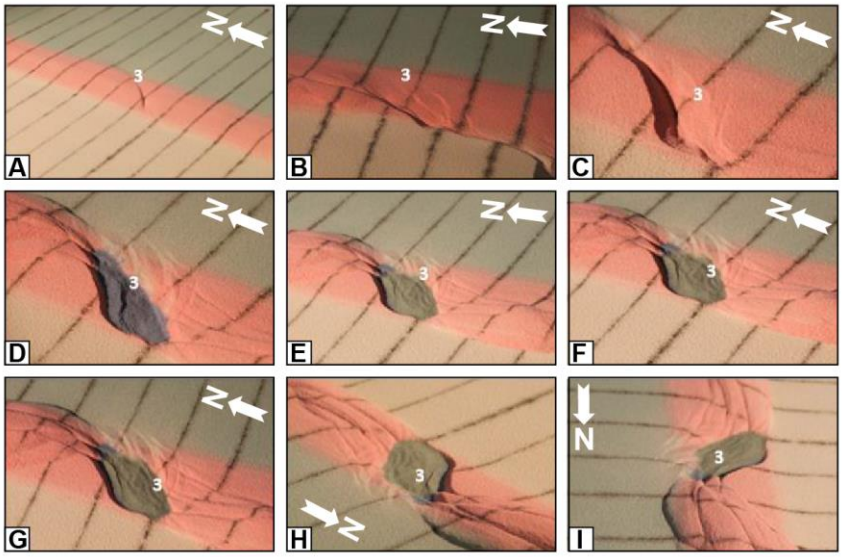

Figure 11: Nine stages in the development of the extensional shear duplex system above the releasing bend in experiment BarMar9. The master faults that developed at an incipient stage (e.g. Fault 3 that constrained the eastern margin of the extensional shear duplex, marked with"3" in the figure; see also **Figure 7**) remained stable and continued to be active throughout the experiment, but became overstepped by new faults in its footwall. These were reactivated as contraction faults at the later stages (stages H and I in this figure). The developing basement was stabilized by infilling of gray sand during this part of the experiment. Fault 3 remained broke through the basin infill also after the basin infill overstepped the original basin margin. The distance between the markers (dark lines) is 5cm. White arrow marks north-direction. Note that figures "H" and "I" (bottom right) is viewed from directions that differs from the other figures.

series "e" and "f" of Mitra & Paul, 2011). Counterparts to PSE-1 structural population were not identified in the seismic data, although some isolated, local anticlinal features could be dismembered remnants of such. Because of their constriction to the near vicinity of the master fault it is reasonable ~~-~~that structures generated at an early stage of shear are vulnerable to cannia~~-~~balization by younger structures with axes striking parallel to the main shear fault (Y-shears; SPE-2-structures). We therefore conclude that thiseis~~-~~ structure population was

764 destroyed during the later stages of shear and during the subsequent stages of
765 extension and contraction.
766 PSE-1-folds, that developed at an incipient stage were immediately
767 pursued by the development of two sets of NNE-SSW-striking normal faults with

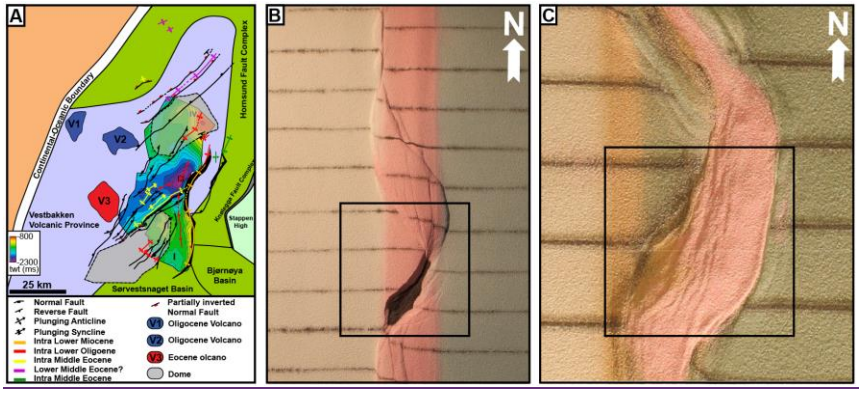

768

769 **Figure 12:** PSE-5-folds generated during phase 3-inversion, experiment BarMar8.
770 Note that fold axes mainly parallel the basin rims, but that they deviate from that
771 in the central parts of the basins in some cases. The folds are best developed in
772 segment 2, which accumulated extension in the combined shear and extension
773 stages.
774

775 opposite throws in the releasing bend areas (e.g. fault 2 **Figure 4**). The two faults
776 defined crescent- or spindle-shaped incipient extensional shear duplexes. These
777 structures were stable during the remainder of the experiments and their master
778 faults became reactivated during the extensional and co~~b~~ntractional phases (see
779 below). The most prominent of these structures corresponds to the position of
780 the Sørvestsnaget Basin (**Figure 1B**).
781 *Segment 2,* which was controlled —by a pre-cut crescent-shaped
782 discontinuity in the experiments corresponds to the Vestbakken Volcanic
783 Province and the southern extension of the Knølegga Fault Complex of the Barents
784 Shear Margin (**Figures 1B~~b~~ and 4**). The Vestbakken Volcanic Province is
785 dominated by interfering NNW-SSE- and NE-SW striking fold- and fault systems
786 in its central part, whereas N-S-structures are more common along its eastern
787 margin (**Figure 12A**) (Jebsen & Faleide, 1998; Gi~~a~~ennenas, 2018). Intra-basinal
788 highs and other internal configurations seen in the BarMar-experiments mainly
789 reflect step-wise collapse of the intrinsic basin that generated rotational fault

blocks, the crests of which separated local ~~s~~sediment accumulations. Such structures are common in strike-slip basins (e.g. Dooley & McClay, 1997; Dooley & Schreurs, 2012) and are consistent with the intra-basin depo-centers seen within the Vestbakken Volcanic province and in the Sørvestsnaget Basin as well (Knutsen & Larsen, 1997; Jebsen & Faleide, 1998; **Figure 13**). The crests of the rotating fault blocks are termed PSE-3-structures above, and such eroded fault block crests are defining the footwalls of major faults in the Vestbakken Volcanic Province, providing space for sediment accumulation in the footwalls. The area that was affected by the basin formation in the extensional shear duplex stage seems to have remained the deepest part of the Vestbakken Volcanic Province, whereas the part formed in basin widening by sequential footwall collapse created a shallower sub-platform (*sensu* Gabrielsen, 1986) (**Figure 11**).

The Knølegga Fault Complex occupies a km-wide zone in segment 2. The master fault strand is paralleled by faults with significant normal throws on its hanging wall side and this belongs to the larger Knølegga Fault Complex (EBF; Eastern Boundary Fault; Giannenas, 2018; **Figure 12A**). The EBF zone is a top-west normal fault with maximum throw of nearly 2000 ms (3000 meters). It can be followed along its strike for more than 60 km and seems to die out by horse-tailing at its tip-points. The vicinity of the master faults of the Knølegga Fault Complex locally display isolated elongate positive structures constrained by steeply dipping faults. These structures sometimes display internal reflection patterns that seem exotic in comparison to the surrounding sequences. Some of these structures resemble positive flower structures or push-ups or define narrow anticlines. They are found in both the footwall and hanging wall of the border faults and strike parallel to those and the axes of these structures parallel the master faults. The traces of such structures can be followed over shorter distances than the master faults, and do not occur in the central parts of the Vestbakken Volcanic Province. We suggest that the composite geometry of the Knølegga Fault Complex is due to the development of PSE-2-structures within the realm of a pre-existing normal fault zone.

Due to the right-stepping geometry during dextral shear in segment 2, the southern and northern parts were in the releasing and restraining bend positions, respectively (e.g. Christie-Blick & Biddle, 1985). Hence, the southern part of

segment 2 was subject to oblique extension, subsidence and basin formation while the northern part was subject to oblique contraction, shortening and uplift. The southern segment expanded to the east and northeast by footwall collapse and

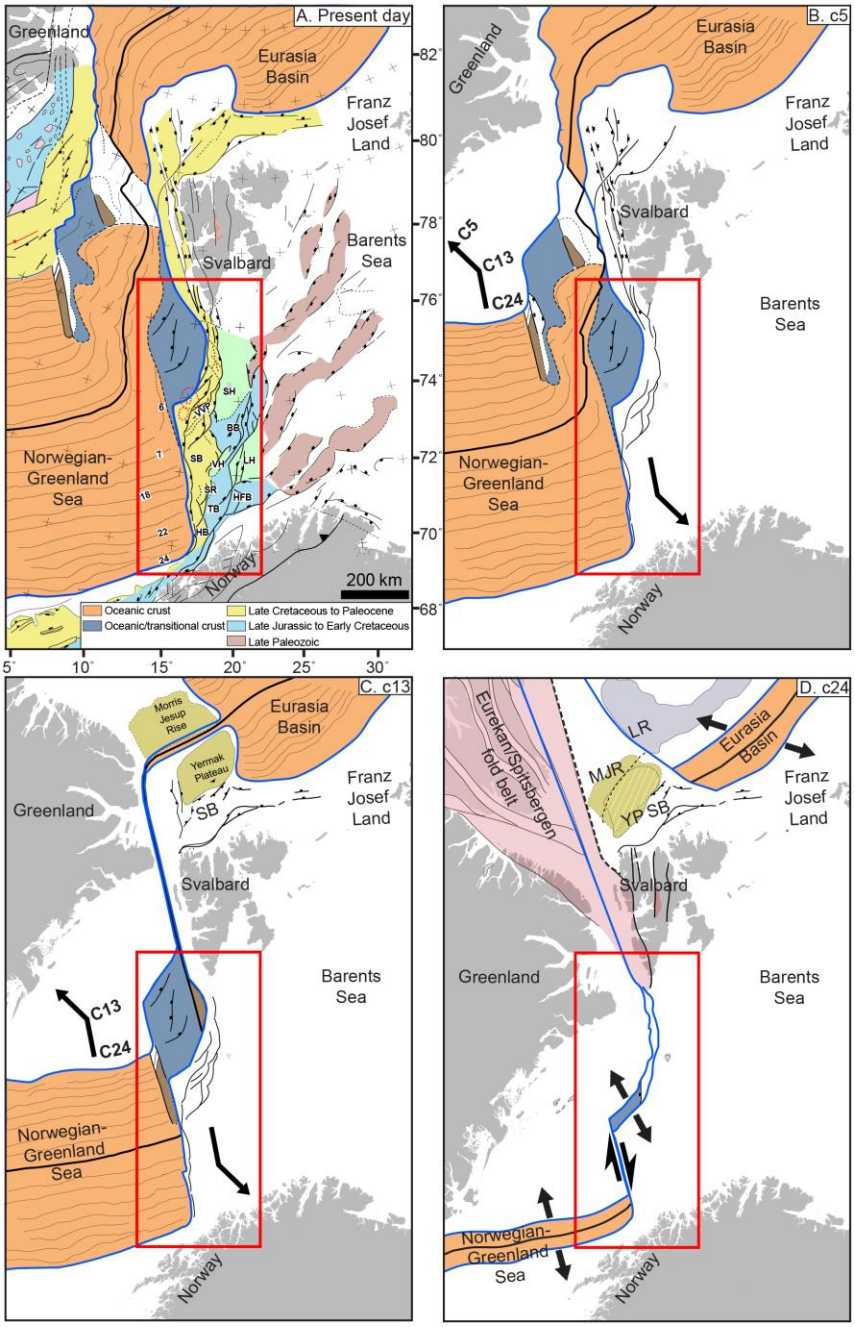

Figure 13: Main stages in opening of the North Atlantic. The figure builds on figure 5 in Faleide et al. (2008) and has been updated and redrawn.

activation of rotating fault blocks that contributed to a basin floor topography that affected the pattern of sediment accumulation (**Figure 9A, B**).

The positive structural elements that prevail in *segment 3* belong to the PSE-2-structure population. The structures affiliated with segment 3 in the BarMar-experiments are similar to those seen in the reflection seismic sections along parts of the Spitsbergen and the Senja shear margins (Myhre, et al. 1982) and elsewhere (Cloos, 1928; Riedel, 1929; Tchalenko, 1970; Wilcox et al., 1973). In the experiments *én echelon* folds (corresponding to PSE-1-structueres) first became visible, to be succeeded by the development of Riedel- and P-shears (R'-shears were subdued as expected for sand-dominated sequences (Dooley & Schreurs, 2012). Continued shear followed by collapse and interaction between Riedel and P-shears and the subsequent development of Y-shears initiated push-up- and flower-structure with N-S-axes (PSE-2) structures that were expressed as non-cylindrical (double-plunging) anticlines on the surface (e.g. Tchalenko, 1970; Naylor et al., 1986). Structures similar to the PSE-2-structures that were initiated in the present experiments are common in scaled experiments with mechanically stratified sequences where viscous basal strata are covered by sand (e.g. Richard et al., 1991; Dauteuil & Mart, 1998).

Structures of phase 2 (extension)

It is expected that (regional) basin and (local) fault block subsidence became accelerated during phase 2 (extension), and more so in the orthogonal extension experiments (BarMar 6) than in the experiments with oblique extension (BarMar 8). However, but due to stabilization of basins by infilling of sand, this was not documented in the final photographs. The widening occurred mainly by fault-controlled collapse of the footwalls, and dominantly along the master faults that corresponded to the Knølegga Fault Complex, but also new intra-basin cross-faults that were initiated in the shear stage (see above) became reactivated, contributing to the complexity of the basin topography. It is not likely that a stage was reached where all (pull-apart) basin units along the margin became fully linked, although sedimentary communication along the margin may have become established.

During the oblique extension stage segment 1 of experiments BarMar7-9 the basin subsidence was focused in the minor pull-apart basins, which soon

Formatted: Indent: First line: 0 cm

865 became linked along the regional N-S-striking basin axis. Remains of several such
866 basin centers, of which the Sørvestsnaget Basin (Knutsen & Larsen, 1997;
867 Kristiansen et al., 2017) is the largest, are preserved and found in seismic data
868 (**Figure 1**B~~b~~). During the experiments a continuous basin system was developed
869 in the hanging wall side of the master fault, ~~.~~ I~~but i~~t is, however, not likely that
870 linking of shear basins occurred prior to the opening stage along the Barents Shear
871 Margin. ~~opening occurred prior to the extension of the margin underlain by~~
872 ~~continental crust reached a stage where the separate basin units paralleling the~~
873 ~~Barents Shear Margin became linked.~~
874 ~~In the subsequent inversion stage, fold populations(PSE-5-folds) with axial traces~~
875 ~~parallel to the basin axis and the master faults characterized segment 1. Remnants~~
876 ~~of such folds are locally preserved in the thickest sedimentary sequences affiliated~~
877 ~~with the Senja Shear Margin.~~
878
879 **Structures of phase 3 (contraction)**
880 The contraction phase (phase 3) ~~clearly~~ reactivated both normal and shear faults
881 in the master fault zone, ~~probably causing~~ also causing ~~focusing of~~ folding in the
882 hanging wall. ~~strain and folding,~~ Simultaneously rotation of (intra-basinal) fault
883 blocks and steepening of pre-existing faults occurred. New fold populations (PSE-
884 5-folds) with axial traces parallel to the basin axis and the master faults
885 characterized the inversion stage. Remnants of such folds are locally preserved in
886 the thickest sedimentary sequences affiliated with the Senja Shear Margin.
887 ~~This means that both intra-basinal and marginal faults in the Vestbakken~~
888 ~~Volcanic Province can have suffered late steepening. Contraction expressed as~~
889 F~~f~~old systems with fold axes paralleling the basin margins as seen in the
890 experiments are also common in the ~~development seems to correspond very well~~
891 ~~to the observed structural configuration of the~~ Vestbakken Volcanic Province. ~~.~~
892 Although shortening occurred inside individual reactivated fault blocks ~~either~~ by
893 large wavelength bulging of the entire sedimentary sequence also trains of folds
894 with larger amplitude and shorter wavelength were developed at this stage
895 (**Figure 12**B,C).
896 Thus, the ~~Here pronounced~~ tectonic inversion was~~is~~ focused along the N-
897 S-striking basin margins but also occurred~~and~~ along some pre-exist~~s~~ing NE-SW-

striking faults and in the central parts of the basin. ~~Pronounced shortening also occurred inside individual reactivated fault blocks either by bulging of the entire sedimentary sequence or as trains of folds (**Figure 12B,C**).~~

During phase 3 the restraining bend configuration in the northern part of segment 2 was characterized by increasing contraction across strike-slip fault strands that splayed out to the northwest from the central part of segment 2 in an early stage of dextral shear. This deformation was terminated by the end of phase 1 by stacking of oblique contraction faults (PSE-5 and PSE-6-structures), defining ~~and~~ an antiformal stack-like structure. This type of deformation falls outside the mapped~~ain~~ area, but to the north this type of oblique shortening during the Eocene (phase 1) was accommodated by regional-scale strain partitioning (Leever et al., 2011a,b).

Also, t~~T~~he Vestbakken Volcanic Province is characterized by extensive regional shortening. Onset of this event of inversion/contraction is dated to early Miocene (Jebsen & Faleide, 1998, Giaennenas, 2018) and this deformation included two main structural fold styles. The first includes upright to steeply inclined closed to open anticlines that are typically present in the hanging wall of master faults. These folds typically have wavelengths in the order of 2.5 to 4.5 kilometers, and amplitudes of several hundred meters. Most commonly they appear with head-on snakehead-structures and are interpreted as buckle folds, albeit a component of shear may occur in the areas of the most intense deformation~~, giving a snake-head-type geometry~~. The second style includes gentle to open anticline-syncline pairs with upright or steep to inclined axial planes ~~open anticlines-synclines~~ with wavelengths in the order of 5 to 7 kilometers and amplitudes of several tens of meters to several hundred meters. We associate those with the PSE-4-type structures as defined in the BarMar-experiments. These folds are situated in positions where sedimentary sequences have been pushed against buttresses provided by master faults along the basin margins. The PSE-6 folds developed as fold trains in the interior basins, where buttressing against larger fault walls was uncommon. Also, this pattern fits well with the development and geometry seen in the BarMar-experiments, where folding started in the central parts of the closing basins before folding of the marginal parts of the basin. In the closing stage the folding and inversion of master faults remained focused along the basin margins.

Formatted: Font color: Auto

The experiments clearly demonstrated that contraction by buckle folding was the main shortening mechanism of the margin-parallel basin system generated in phase 2 (orthogonal or oblique extension) in all segments. In the Vestbakken Volcanic Province segments of the Knølegga Fault Complex, the EBF and the major intra-basinal faults contain clear evidence for tectonic inversion, whereas this is less pronounced in others. The hanging wall of the EBF is partly affected by fish-hook-type inversion anticlines (Ramsey & Huber, 1987; Griera et al., 2018) (**Figure 2D,-E**), or isolated hanging wall anticlines or pairs or trains of synclines and anticlines (e.g.; Roberts, 1989; Coward et al., 1991; Cartwright, 1989; Mitra, 1993; Uliana et al., 1995; Beauchamp et al. 1996; Gabrielsen et al. 1997; Henk & Nemcok 2008), the fold style and associated faults probably being influenced by the orientation and steepness of the pre-inversion fault (Williams et al., 1989; Cooper et al., 1989; Cooper & Warren, 2010). Some structures of this type can still be followed for many kilometers having consistent geometry and attitude. These structures have not been much modified by reactivation and are invariably found in the proximal parts footwalls of master faults, suggesting that these are inversion structures. They– correlate to PSE-type 5-structures in the experiments that developed in areas of focused contraction along pre-existing fault scarps during Oligocene inversion.

Trains of folds with smaller amplitudes and higher frequency are sometimes found in fault blocks in the central part of the Vestbakken Volcanic Province (**Figure 12A**). Although these structures are not dateable ~~m~~by seismic stratigraphical methods (on-lap configurations etc.) we regard these fold strains to be correlatable with the tight folds generated in the inversion stage in the experiments (PSE-6-structures) and that they are contemporaneous with the PSE-5-structures.

Segment 1 in the experiments, that corresponds to the Senja Shear Margin ~~segment~~, displays a structural pattern that is a hybrid between segments 1 and 2: It contains incipient structural elements that were developed in full in segments 2 and 3, segment 2 being dominated by releasing and restraining bend configurations and segment 3 dominated by neutral shear. Due to internal configurations, the three segments were affected to secondary (oblique) opening

and contraction in various fashions. Understanding these differences was much promoted by the comparison of seismic and model data.

Some considerations about multiphase deformation in shear margins

The Barents Shear Margin is a challenging target for structural analysis both because it represents a geometrically complex structural system with a multistage history, but also because high-quality (3D) reflection seismic data are limited and many structures and sedimentary systems generated in the earlier tectonothermal stages have been overprinted and obliterated by younger events. This makes analogue experiments very useful in the analysis, since they offer a template for what kind of structural elements can be expected. By constraining the experimental model according to the outline of the margin geometry and imposing a dynamic stress model in harmony according to the state-of-the-art knowledge about the regional tectono-sedimentological development, we were able to interpret the observations done in reflection seismic data in a new light.

Continental margins are commonly segmented containing primary or secondary transform elements, and pure strike-slip transforms are relatively rare (e.g. Nemcok et al. 2016). Such margins, however, invariably become affected by extension following break-up and sometimes contraction due to ridge-push or far-field stress perhaps related to plate reorganization. The complexity of shear margins has ignited several conceptual discussions. One such discussion concerns the presence of zones of weakness prior to break-up (e.g. Sibuet & Mascle 1978; Taylor et al, 2009; Gibson et al. 2013; Basile 2015). In the case of the Barents Shear Margin the de Geer zone provides such a pre-existing zone of weakness, and this premise was acknowledged when the scaled model was established. The relevance of our model is therefore constrained to cases where a crustal-scale zone of weakness existed before break-up. Furthermore, in cases with pre-existing zones of weakness, our model demonstrates that the incipient architecture of the margin is important indeed and the detailed geometry and width of the pre-existing week zone must be mapped and included in the model.

Summary and conclusions

Our observations confirmed that the main segments of the Barents Shear Margin, albeit undergoing the same reginal stress regime, display contrasting structural configurations. The deformation in segment 2 in the BarMar-experiments, was determined by releasing and restraining bends in the southern and northern parts, respectively. Thus, the southern part, corresponding to the Vestbakken Volcanic Province, was dominated by the development of a regional-scale extensional shear duplex as defined by Woodcock & Fischer (1983) and Twiss & Moores (2007). By continued shear the basin developed into a full-fledged pull-apart basin or rhomb graben (Crowell, 1974; Aydin & Nur, 1982) in which rotating fault blocks were trapped. The pull-apart-basin became the nucleus for greater basin systems to develop in the following phase of extension also providing the space for folds to develop in the contractional phase.

We conclude that fault- and fold systems found in the realm of the Vestbakken Volcanic Province are in accordance with a three-stage development that includes dextral shear followed by oblique extension and contraction ($315/135^0$) along a shear margin with composite geometry.

Folds with NE-SW-trending fold axes ~~that~~ are dominant in wider area of the Vestbakken Volcanic Province and are dominated by folds in the hanging walls of (older) normal faults, sometimes characterized by narrow, snake-head- or harpoon-type structures that are typical for tectonic inversion (Cooper et al., 1989; Coward, 1994; Allmendinger, 1998; Yameda & McClay, 2004; Pace & Calamitra, 2014) ~~typical of inverted faults~~.

Comparing seismic mapping and analogue experiments it is evident that a main challenge in analyzing the structural pattern in shear margins of complex geometry and multiple reactivation is the low potential for preservation of structures that were generated in the earliest stages of the development.

Author contribution

R.H.Gabrielsen: Contributions to outline, design and performance of experiments. First writing and revisions of manuscript. First drafts of figures.

P.A.Giannenas: Seismic interpretation in the Vestbakken Volcanic Province. Identification and description of fold families.

Suggestion:

D.Sokoutis: Main responsibility for set-up, performance and handling of experiments. Revisions of manuscript.

E.Willigshofer: Performance and handling of experiments. Revisions of manuscript. Design and revisions of figure material.

M. Hassaan: Background seismic interpretation. Discussions and revisions of manuscript. Design and revisions of figure material.

J.I.Faleide: Regional interpretations and design of experiments. Participation in performance and interpretations of experiments. Revisions of manuscript, design and revisions of figure material.

Acknowledgements

The work was supported by ARCEx (Research Centre for Arctic Petroleum Exploration), which was funded by the Research Council of Norway (grant number 228107) together with 10 academic and six industry (Equinor, Vår Energi, Aker BP, Lundin Energy Norway, OMV and Wintershall Dea) partners. Muhammad Hassaan was funded by the Suprabasins project (Research Council of Norway grant no. 295208). We thank to Schlumberger for providing us with academic licenses for Petrel software to do seismic interpretation. Two anonymous reviewers and the editors of this special volume provided comments, suggestions and advice that enhanced the clarity and scientific quality of the paper.

~~**Author contribution**~~

~~R.H. Gabrielsen: Contributions to outline, design and performance of experiments. First writing and revisions of manuscript. First drafts of figures.~~

~~P.A. Gjaennenas: Seismic interpretation in the Vestbakken Volcanic Province. Identification and description of fold families.~~

~~Suggestion:~~

~~D. Sokoutis: Main responsibility for set-up, performance and handling of experiments. Revisions of manuscript.~~

~~E. Willigshofer: Performance and handling of experiments. Revisions of manuscript. Design and revisions of figure material.~~

~~Md. Hassaan: Background seismic interpretation. Discussions and revisions of manuscript. Design and revisions of figure material.~~

~~J.I. Faleide: Regional interpretations and design of experiments. Participation in performance and interpretations of experiments. Revisions of manuscript, design and revisions of figure material.~~

Acknowledgements

Muhammad Hassaan was funded by the Suprabasins project (Research Council of Norway grant no. 295208). We thank Schlumberger for providing us with academic licenses for Petrel software to do seismic interpretation.
Two anonymous reviewers and the editors of this special volume provided comments, suggestions and scientific and linguistic advice on several revisions of this paper that enhanced itsthe clarity and scienific quality. of the paper.

FIGURES

Figure 1: A) The Barents Sea provides is separated from the Norwegian-Greenland Sea by the de Geer transfer margin. Red box shows the present study area. **B)** Structural map Barents Sea shear margin. Note segmentation of the continent-ocean transition. Abbreviations (from north to south): WSFTB = West Spitsbergen Fold-and-Thrust Belt, HFZ = Hornsund Fault Complex, KFC = Knølegga Fault Zone, VVP = Vestbakken Volcanic Province, SB = Sørvestsnaget Basin, VH = Veslemøy High, SR = Senja Ridge, SSM = Senja Shear Margin. Blue lines indicate position of seismic profiles in Figure 2 and red line X-X´ shows western border of thinned crust (see also Figure 3). Chron numbers are indicated on oceanic crust area.

Figure 2: Seismic examples, Vestbakken Volcanic Province. **A)** Gentle, partly collapsed NE-SW-striking anticline/dome of uncertain origin in the eastern terrace domain of the southern Vestbakken Volcanic Province. **B,C)** Asymmetrical folds (fold family 2; Giannenas 2018) situated along the eastern margin of the Vestbakken Volcanic Province. These may represent primary SPE-4 structures focused in the hangingwalls along margins of master fault blocks, representing reactivated SPE-2 structures. **D)** trains of symmetrical folds with upright fold axes (corresponding to PSE-5 structures) are preserved inside larger fault blocks. See text for explanation of SPE structures. **E)** Section through push-up associated with restraining bend (PSE-4 structure). **F)** Flower (PSE-2) structure in aera dominated by neutral shear.

Figure 3: A) Schematical set-up of BarMar3 experiment as seen in map view. **B)** Section through same experiment before deformation, indicating stratification and thickness relations. **C)** Standard positions and orientation for sections cut in all experiments in the BarMar series. Yellow numbers are section numbers. Black numbers indicate angle between the margins of the experiment (relative to N-S) for each profile. **D)** Outline of silicone putty layer as applied in all experiments. Inset shows original structural map of the Barents Margin used to define the width of the thinned crust. Red line (X-X') indicates the western limit of the thinned zone.

Figure 4: Position of segments and major structural elements as referred to in the text and subsequent figures (see particularly **Figures 5 and 6**). This example is taken from the reference experiment BarMar6. All experiments BarMar6-9 followed the same pattern, and the same nomenclature was used in the description of all experiments and provides the template for the definition of structural elements in **Figure 7**.

Figure 5: Sequential development of experiment BarMar6 by 0.5, 2.4, 3.5, 4.0 and 5.0 cm of dextral shear (Steps A-E), orthogonal extension (steps F-H) and oblique contraction (steps I-J). The master fault strands are numbered in **Figure 4**, and the sequential development for each structural family is shown in **Figure 7**. The reference panel to the upper left shows the positions of the segments.

Figure 6: Sequential development of experiment BarMar8 by 0.5, 2.4, 3.5, 4.0 and 5.0 cm of dextral shear (Steps A-E), oblique extension (steps F-H) and oblique

Formatted: Font: Bold

contraction (steps I-J). The master fault strands are numbered in **Figure 3**, and the sequential development for each structural family is shown in **Figure 7**. Phases 2 and 3 involved oblique (315^0) extension and contraction in this experiment. The reference panel to the upper left shows the positions of the segments.

Figure 7: Summary of sequential activity in each master fault in Experiment BarMar6 (**Figure 5**) (for position of each fault, see **Figure 4**). Type and amount of displacement is shown in two upper horizontal rows. The vertical blue bar indicates the stage at which full along-strike communication became established between marginal basins. Color code (see in-set) indicates type of displacement at any stage. The reference panel to the left shows the positions of the segments.

Figure 8: PSE-1 anticline-syncline pairs in segment 1 of experiment BarMar6 in an oblique view. (see **Figure 4** for position of Segment 1). PSE-1 folds (indicated by relief defined by blue and yellow markers) were constrained to the centralvery fault zone (defined by Y-shear and its splay faults), and the fold axes (blue lines) and extended only 3-4 cm beyond itthe fault zone. PSE-2 structures (incipient push-ups and positive flower structures); yellow lines) were delineated by shear faults (black lines) and completely cannibalized PSE-1 structures by continued shear. . Yellow and blue reference lines illustrateshow the rotation of the fold axial trace caused by dextral shearing. of c. 1,5 cm. 25mm of dextral shear. Already By a displacement of 35mm the remains of the PSE-1 structure was completely obliterated. Ppre-shearThe distance between the markers (blue and yellowdark lines) was is 5cm.
Black arrow indicates shear direction.
Yellow arrow marks north direction.
White arrows indicate shear direction.

Figure 9: Cross sections through PSE-2 related structures. PSE structures are marked with P and PSE-number as described in text (see also Table 1). **A)** Folded core of incipient push-up/positive flower structure in segment 1, experiment BarMar6. The fold structure is completely enveloped of shear faults that have a twisted along-strike geometry. Note that the eastern margin of the structure developed into a negative structure at a late stage in the development (filled by black-pink sand sequence) and that the silicone putty sequence (basal pink sequence) was entirely isolated in the footwall. **B)** Similar structure type in experiment BarMar8. However, tThe basal weak silicone putty layer here bridged the basal high-strain zone so that folding occurred in the footwall as well as in the hanging. and focused Ffoldsing that propagated up-section into the sand layers (blue). The folds in upper (pink) layers) are younger and were associated with the contractional stage (PSE-6 structures)., because they contributed to a surface relief filled in by red-black sand sequence that was sieved into the margin during the contractional stage. **C)** Contraction associated with "crocodile structure" in the footwall of the main fault in segment 1, experiment BarMar8. Note disharmonic folding with contrasting fold geometries in hanging wall and footwall and at

Formatted: Font: Bold

different stratigraphic levels in the footwall, indicating that shifting stress situation in time and space occurred in the experiment. **D)** Transitional fault strand between to more strongly sheared fault segments (experiment BarMar9).

Figure 10: A) contrasting structural styles along the master fault system in segment 2 in map view and **(B)** cross sections of experiment BarMar9. SL denotes silicone layer, the stippled line the boundary between pre- and syn-deformation layers and the white dashed line the boundary with the post-deformation layers.

Figure 11: Nine stages in the development of the extensional shear duplex system above the releasing bend in experiment BarMar9. The master faults that developed at an incipient stage (e.g. Fault 3 that constrained the eastern margin of the extensional shear duplex, marked with"3" in the figure; see also **Figure 7**) remained stable and continued to be active throughout the experiment. (Figure 7), but became overstepped by new faults in its footwall. These were recrivatedreactivated as that became the basin contraction faults at the later stages (stages H and I in this figure). The developing basement was stabilized by infilling of gray sand during this part of the experiment. Fault 3 remained active and broke through the basin infill also after the basin infill overstepped the original basin margin. The distance between the markers (dark lines) is 5cm. White Yellow arrow marks north direction. Note that figures "H" and "I" (bottom right) is viewed from directions that differs from the other figures.

Figure 12: PSE 5 folds generated during phase 3 inversion, experiment BarMar8. Note that fold axes mainly parallel the basin rims, but that they deviate from that in the central parts of the basins in some cases. Thehe folds are best developed in segment 2, which accumulated extension in the combined shear and extension stages.

Figure 13; Main stages in opening of the North Atlantic. The figure builds on figure 5 in Faleide et al. (2008) and has been updated and redrawn.

Table 1: Characteristics of Positive Structural Element (PSE 1-6) as described in the text and shown in figures. Note that the PSE-1-structures that were developed in the earliest stages of the experiments became cannibalized during the continued deformation. No candidates of these structures were identified in the reflection seismic sections.

Formatted: Font: Bold

References

Allemand P. and Brun J.P.: Width of continental rifts and rheological layering of the lithosphere. Tectonophysics, 188, 63-69, 1991.

Allmendinger,R.W.: : Inverse and forward numerical modeling of threeshear fault-propagation folds, Tectonics, 17(4), 640-656, 1998.

Auzemery, A., E. Willingshofer, D. Sokoutis, J.P. Brun and Cloetingh S.A.P.L.,: Passive margin inversion controlled by stability of the mantle lithosphere, Tectonophysics, 817, 229042, 1-17, https://doi.org/10.1016/j.tecto.2021.229042, 2021.

Aydin,A. and Nur,A.:1982: Evolution of pull-apart basins and their scale independence. Tectonics, 1, 91-105, 1982.

Ballard J-F., Brun J-P. and Van Ven Driessche J.: Propagation des chevauchements au-dessus des zones de décollement: modèles expérimentaux. Comptes Rendus de l'Académie des Sciences, Paris, 11, 305, 1249-1253, 1987.

Basile, C.: Transform continental margins – Part 1: Concepts and models. Tectonophysics, 661, pp.1-10. doi: 10.1016/j.tecto.2015.08.034, 2015.

Basile,C. and Brun,J.-P.: Transtensional faulting patterns ranging from pull-apart basins to transform continental margins: an experimental investigation, Journal of Structural Geology, 21,23-37, 1997.

Beauchamp,W., Barazangi,M., Demnati,A. and El Alji,M.: Intracontinental rifting and inversion: Missour Basin and Atlas Mountains, Morocco. American Association of Petroleum Geologists Bulletin, 80(9), 1455-1482, 1996.

Bergh,S.G., Braathen,A. and Andresen,A.: Interaction of basement-involved and thin-skinned tectonism in the Tertiary fold-and-thrust belt of Central Spitsbergen, Svalbard. American Association of Petroleum Geologists Bulletin, 81(4), 637-661,1997.

Bergh,S.G. and Grogan,P.: Tertiary structure of the Sørkapp-Hornsund Region, South Spitsbergen, and implications for the offshore southern extension of the fold-thrust-belt. Norwegian Journal of Geology, 83, 43-60, 2003.

Biddle, K.T. and Christie-Blick, N., (eds.): Strike-Slip Deformation, Basin Formation, and Sedimentation: Society of Economic Paleontologists and Mineralogists Special Publication, 37, 386pp, 1985a.

Biddle, K.T. and Christie-Blick, N.: Glossary — Strike-slip deformation, basin formation, and sedimentation, in: Biddle, K.T., and Christie-Blick, N. (eds.): Strike-Slip Deformation, Basin Formation, and Sedimentation: Society of Economic Paleontologists and Mineralogists Special Publication, 37, 375-386, 1985b

Blaich,O.A., Tsikalas,F. and Faleide,J.I.: New insights into the tectono-stratigraphic evolution of the southern Stappen High and the transition to Bjørnøya Basin, SW Barents Sea, Marine and Petroleum Geology, 85, 89-105, doi: 10.1016/j.marpetgeo.2017.04.015, 2017.

Breivik,A.J., Faleide,J.I. and Gudlaugsson,S.T.: Southwestern Barents Sea margin: late Mesozoic sedimentary basins and crustal extension, Tectonophysics, 293, 21-44, 1998.

Breivik,A.J., Mjelde,R., Grogan,P., Shinamura,H., Murai,Y. and Nishimura,Y.: Crustal structure and transform margin development south of Svalbard based on ocean bottom seismometer data. Tectonophysics, 369, 37-70 2003.

Brekke, H.: The tectonic evolution of the Norwegian Sea continen- tal margin with emphasis on the Vøring and Møre basins: Geological Society, London, Special Publication, 136, 327–378, 2000.

Brekke, H. and Riis, F.: Mesozoic tectonics and basin evolution of the Norwegian Shelf between 60˚N and 72˚N. Norsk Geologisk Tidsskrift, 67, 295-322, 1987.

Burchfiel, B.C. and Stewart,J.H.: "Pull-apart" origin of the central segment of Death Valley, California. Geological Society of America Bulletin, 77, 439-442, 1966.

Campbell,J.D.: *En échelon* folding, Economical Geology, 53(4), 448-472, 1958.

Cartwright,J.A.: The kinematics of inversion in the Danish Central Graben. in: M.A.Cooper & G.D.Williams (eds.): Inversion Tectonics. Geological Society of London Special Publication, 44, 153-175, 1989.

Casas, A.M., Gapals,D., Nalpas,T., Besnard,K. and Román-Berdiel,T.: Analogue models of transpressive systems, Jornal of Structural Geology, 23,733-743, 2001

Christie-Blick,N. and Biddle,K.T.: Deformation and basin formation along strike-slip faults. in: Biddle,K.T. & Christie-Blick,N. (eds.): Strike-slip deformation, basin formation and sedimentation. Society of Economic Mineralogists and Palaeontologists (Tulsa Oklahoma), Special Publication, 37, 1-34, 1985.

Cloos,H.: Experimenten zur inneren Tectonick, Zentralblatt für Mineralogie, Geologie und Palaentologie, 1928B, 609-621, 1928.

Cloos,H.: Experimental analysis of fracture patterns, Geological Society of America Bulletin, 66(3), 241-256, 1955.

Cooper,M. and Warren,M.J.: The geometric characteristics, genesis and petroleum significance of inversion structures, in Law,R.D., Butler,R.W.H., Holdsworth,R.E., Krabbendam,M. & Strachan,R.A. (eds.): Continental Tectonics and Mountain Building: The Lagacy of Peache and Horne, Geological Society of London, Special Publication, 335, 827-846, 2010.

Cooper,M.A., Williams,G.D., de Graciansky,P.C., Murphy,R.W., Needham,T., de Paor,D., Stoneley,R., Todd,S.P., Turner,J.P. and Ziegler,P.A.: Inversion tectonics – a discussion. Geological Society, London, Special Publications, 44, 335-347, 1989.

Coward, M.: Inversion tectonics, in: Hancock,P.L. (ed.): Continental Deformation, Pergamon Press, 289-304, 1994.

Coward, M.P., Gillcrist, R. and Trudgill, B.: Extensional structures and their tectonic inversion in the Western Alps, *in*: A.M.Roberts, G.Yielding & B.Freeman (eds.): The Geometry of Normal Faults. Geological Society of London Special Publication, 56, 93-112 1991.

Crowell, J.C.: Displacement along the San Andreas Fault, California, Geological Society of America Special Papers, 71, 59pp, 1962.

Crowell, J.C.: Origin of late Cenozoic basins in southern California. in Dorr, R.H. and Shaver, R.H. (eds.): Modern and ancient geosynclinal sedimentation. SEPM Special Publication, 19, 292-303, 1974a

Crowell, J.C., 1974b: Implications of crustal stretching and shortening of coastal Ventura Basin, *in:* Howell,D.G. (ed.): Aspects of the geological history of the Calefornia continental Borderland, American Association of Petroleum Geologists, Pacific Section,Publication, 24, 365-382, 1974b

Cunningham, W.D. and Mann, P. (eds.): : Tectonics of Strike-Slip Restraining and Releasing Bends, Geological Society London Special Publication, 290, 482pp, 2007a.

Cunningham, W.D. and Mann, P.: Tectonics of Strike-Slip Restraining and Releasing Bends, *in:* Cunningham,W.D. & Mann,P. (eds.), 2007: Tectonics of Strike-Slip Restraining and Releasing Bends, Geological Society London Special Publication, 290, 1-12, 2007b.

Dauteuil, O. and Mart, Y.: Analogue modeling of faulting pattern, ductile deformation, and vertical motion in strike-slip fault zones, Tectonics, 17(2), 303-310, 1998.

Del Ventisette, C., Montanari, D., Sani, F., Bonini, M. and Corti, G.: Reply to comment by J. Wickham on ‘‘Basin inversion and fault reactivation in laboratory experiments’’. Journal of Structural Geology 29, 1417–1418, 2007.

Dooley, T. and McClay, K.: Analog modeling of pull-apart basins, American Association of Petroleum Geologists Bulletin, 81(11), 1804-1826, 1997.

Dooley, T.P. and Schreurs, G.:Analogue modelling of intraplate strike-slip tectonics: A review and new experimental results, Tectonophysics, 574-575, 1-71, 2012

Doré, A.G. and Lundin, E.R.: Cenozoic compressional structures on the NE Atlantic margin: nature, origin and potential significance for hydrocarbon exploration. Petroleum Geosciences, 2, 299-311, 1996

Doré, A.G., Lundin, E.R., Gibbons, A., Sømme, T.O. and Tørudbakken, B.O.: Transform margins of the Arctic: a synthesis and re-evaluation *in:* Nemcok,M., Rybár,S., Sinha,S.T., Hermeston,S.A. & Ledvényiová,L. (eds.): Transform Margins,: Development, Control and Petroleum Systems, Geological Society London, Special Publication, 431, 63-94, 2016.

Doré, A.G., Lundin, E.R., Jensen, L.N., Birkeland, Ø., Eliassen, P.E. and Fichler, C.: Principal tectonic events in the evolution of the northwest European Atlantic margin. In: A.J.Fleet & S.A.R.Boldy (eds.): Petroleum Geology of Northwest Europe: Proceedings of the Fifth Conference (Geological Society of London), 41-61, 1999.

Eidvin, T., Goll, R.M., Grogan, P., Smelror, M. and Ulleberg, K.: The Pleistocene to Middle Eocene stratigraphy and geological evolution of the western Barents Sea continental margin ta well site 731675-1 (Bjørnøya West area). Norsk Geologisk Tidsskrift, 78, 99-123 1988.

Eidvin, T., Jansen, E. and Riis,F.: Chronology of Tertiary fan deposits off the western Barents Sea: Implications for the uplift and erosion history of the Barents Shelf. Marine Geology, 112, 109-131, 1993.

Eldholm, O., Faleide, J.I. and Myhre, A.M.: Continent-ocean transition at the western Barents Sea/Svalbard continental margin. Geology, 15, 1118-1122, 1987.

Eldholm, O., Thiede, J., and Taylor, E.: Evolution of the Vøring volcanic margin, *in:* Eldholm, O., Thiede, J., and Taylor, E., (eds.): Proceedings of the Ocean Drilling

Program, Scientific Results, 104: College Station (Ocean Drilling Program), TX, 1033–1065, 1989.

Eldholm, O., Tsikalas, F. and Faleide,J.I.: Continental margin off Norway 62-75°N:Paleogene tectono-magmatic segmentation and sedimentation. Geological Society of London Special Publication, 197, 39-68, 2002

Emmons, R.C.: Strike-slip rupture patterns in sand models, Tectonophysics, 7, 71-87, 1969.

Faugère, E., Brun, J.-P. and Van Den Driessche, J.: Bassins asymmétriques en extension pure et en détachements:Modèles expérimentaux, Bulletin Centre Recherche Exploration et Production Elf Aquitaine, 10(2), 13-21, 1986.

Faleide, J.I., Bjørlykke, K. and Gabrielsen, R.H.: Geology of the Norwegian Shelf. *in*: Bjørlykke,K.: Petroleum Geoscience: From Sedimentary Environments to Rock Physics 2nd Edition, Springer-Verlag, Berlin Heidelberg, Chapter 25, 603 -637, 2015.

Faleide, J.I., Myhre, A.M. and Eldholm, O.: Early Tertiary volcanism at the western Barents Sea margin. in: A.C.Morton & L.M.Parsons (eds.): Early Tertiary volcanism and the opening of the NE Atlantic.Geological Society of London Special Publication, 39,135-146, 1988.

Faleide, J.I., Tsikalas, F., Breivik, A.J, Mjelde, R., Ritzmann, O., Engen, Ø., Wilson, J. and Eldholm, O.: Structure and evolution of the continental margin off Norway and the Barents Sea. Episodes, 31(1), 82-91, 2008.

Faleide, J.I., Vågnes, E. and Gudlaugsson, S.T.:: Late Mesozoic - Cenozoic evolution of the south-western Barents Sea in a regional rift-shear tectonic setting. Marine and Petroleum Geology, 10, 186-214, 1993

Fichler, C. and Pastore, Z.: Petrology and crystalline crust in the southwestern Barents Sea inferred from geophysical data. Norwegian Journal of Geology, 102, 41pp, https://dx.doi.org/10.17850/njg102-2-2, 2022.

Freund, R.: The Hope Fault, a strike-slip fault in New Zealand, New Zealand Geological Survey Bulletin, 86, 1-49, 1971.

Gabrielsen, R.H.: Structural elements in graben systems and their influence on hydrocarbon trap types. in: A.M. Spencer (ed.): Habitat of Hydrocarbons on the Norwegian Continental Shelf. Norw. Petrol. Soc. (Graham & Trotman), 55 – 60, 1986.

Gabrielsen, R.H., Færseth, R.B., Jensen, L.N., Kalheim, J.E. and Riis, F.: Structural elements of the Norwegian Continental Shelf. Part I: The Barents Sea Region. Norwegian Petroleum Directorate, Bulletin, 6, 33pp, 1990.

Gabrielsen, R.H., Grunnaleite, I. and Rasmussen, E.: Cretaceous and Tertiary inversion in the Bjørnøyrenna Fault Complex, south-western Barents Sea. Marine and Petroleum Geology, 142, 165-178, 1997.

Gac, S., Klitzke, P., Minakov, A.,, Faleide. J.I. and Scheck-Wenderoth, M.,: Lithospheric strength and eleastic thickness of the Barents Sea and Kara Sea region, Tectonophysics, 691, 120-132, doi: 10.106/j.tecto.2016.04.028, 2016.

Gaina, C., Gernigon, L. and Ball.P.: Palaeocene – Recent plate boundaries in the NE Atlantic and the formation of the Jan Mayen microcontinent. Journal of the Geological Society, London, 166(4), 601-616, 2009.

Ganerød, M., Smethurst, M.A., Torsvik, T.H., Prestvik, T., Rousse, S., McKenna, C., van Hinsberen, D.J.J. and Hendriks, W.W.H.: The North Atlantic Igneous Province reconstructed and its relation to the Plume Generation Zone: the Antrim Lava Group revisited. Geophysical Journal International, 182, 183-202, doi: 10.1111/j.1365-246X.2010.04620.x, 2010.

Giannenas, P.A.: The Structural Development of the Vestbakken Volcanic Province, Western Barents Sea. Relation between Faults and Folds, Unpublished Ms.Sci.thesis, University of Oslo, 89 pp., 2018

Gibson, G.M., Totterdell, J.M., White,N. Mitchell, C.H., Stacey,A.R., M. P. Morse, M.P. and A. Whitaker: Preexisting basement structures and its influence on continental rifting and fracture development along Australia's southern rifted margin, Journal of the Geological Society of London, 170, 365-377, 2013.

~~Giennenas, P.A.: The Structural development of the Vestbakken Volcanic Province, Western Barents Sea. Relation between Ffaults and folds, Unpubl. Master thesis, University of Oslo 2018, 89 pp, 2018~~.

Graymer, R.W., Langenheim, V.E., Simpson, R.W., Jachens, R.C. and Ponce, D.A.: Relative simple through-going fault planes at large-earthquake depth may be concealed by surface complexity of strike-slip faults, *in*: Cunningham,W.D. & Mann,P. (eds.): Tectonics of Strike-Slip Restraining and Releasing Bends, Geological Society London Special Publication, 290, 189-201, 2007.

Griera, A., Gomez-Rivas, E. and Llorens,M.-G.: The influence of layer-interface geometry of single-layer folding. Geological Society of London Special Publication 487, SP487:4, 2018.

Grogan, P., Østvedt-Ghazi, A.-M., Larssen, G.B., Fotland, B., Nyberg, K., Dahlgren, S. and Eidvin, T.: Structural elements and petroleum geology of the Norwegian sector of the northern Barents sea. *in*: Fleet,A.J. & Boldry,S.A.R. (eds.): Petroleum Geology of Northwest Europe: Proceedings of the 5th Conference, Geological Society of London, 247-259, 1999.

Groshong, R.H.: Half-graben structures: balanced models of extensional fault bend folds, Geological Society of America Bulletin, 101, 96-195, 1989

Gudlaugsson, S.T. and Faleide, J.I.: The continental margin between Spitsbergen & Bjørnøya, in: O.Eiken (ed.): Seismic Atlas of Western Svalbard, Norsk Polarinstitutt Meddelelser, 130, 11-13, 1994.

Gudlaugsson, S.T., Faleide, J.I., Johansen, S.E. and Breivik, A.J.: Late Palaeozoic structural development of the south-western Barents Sea. Marine and Petroleum Geology, 15, 73-102, 1998.

Hamblin, W.K.: Origin of "reverse drag" on the down-thrown side of normal faults, Geological Society of America Bulletin, 76, 1145-1164,. 1965.

Hanisch, J.: The Cretaceous opening of the Northeast Atlantic. Tectonophysics, 101, 1-23, 1984.

Harding, T.P.: Petroleum traps associated with wrench faults. American Association of Petroleum Geologists Bulletin, 58, 1290-1304, 1974.

Harding, T.P. and Lowell, J.D.: Structural styles, their plate tectonic habitats, and hydrocarbon traps in petroleum provinces, American Association of Petroleum Geologists Bulletin, 63,1016-1058, 1979.

Harland, W.B.: The tectonic evolution of the Arctic-North Atlantic Region, in: Taylor,J.H., Rutten,M.G., Hales,A.L., Shackelton,R.M., Nairn,A.E. & Harland:W.B.,: Discussion, A Symposium on Continental Drift, Philosophical Transactions of the Royal Society of London,, Series A, 258, 1088, 59-75, 1965.

Harland, W.B.: Contributions of Spitsbergen to understanding of tectonic evolution of North Atlantic Region, American Association of Petroleum Geologists, Memoir 12, 817-851, 1969.

Harland, W.B.: Tectonic transpression in Caledonian Spitsbergen, Geological Magazine, 108, 27-42, 1971

Henk, A. and Nemcok, M.: Stress and fracture prediction in inverted half-graben structures. Journal of Structural Geology, 30(1), 81-97, 2008.

Horni, J.Á., Hopper, J.R., Blischke, A., Geisler, W.H., Stewart, M., Mcdermott, K., Judge, M., Erlendsson, Ö. and Árting, U.E.: Regional Distribution of Volcanism within the North Atlantic Igneous Province. The NE Atlantic Region: A Reappraisal of Crustal Structure, Tectonostratigraphy and Magmatic Evolution. Geological Society, London, Special Publications, 447, 105–125, https://doi.org/10.1144/SP447.18, 2017.

Horsfield, W.T., 1977: An experimental approach to basement-controlled faulting. Geologie en Mijbouw, 56(4), 3634-370 1977.

Hubbert, M.K.: Theory of scale models as applied to the study of geologic structures, Bulletin Geological Society of America, 48, 1459-1520, 1937.

Jebsen, C. and Faleide, J.I.: Tertiary rifting and magmatism at the western Barents Sea margin (Vestbakken volcanic province). III international conference on Arctic margins, ICAM III; abstracts; plenary lectures, talks and posters, 92. 1998.

1589 Khalil,S.M. and McClay,K.R.: 3D geometry and kinematic evolution of extensional
1590 fault-related folds, NW Red Sea, Egypt. in: Childs,C., Holdswort,R.E., Jackson,C.A.L.,
1591 Manzocchi,T., Walsh,J.J & Yielding,G. (eds.): The Geometry and Growth of Normal
1592 Faults, Geological Society, London, Special Publication 439,
1593 doi.org/10.1144/SP439.11, 2016.
1594
1595 Klinkmüller, M., Schreurs, G., Rosenau, M. and Kemnitz, H.: Properties of
1596 granular analogue model materials: a community wide survey. Tectonophysics
1597 684, 23–38. http://dx.doi.org/10.1016/j.tecto.2016.01.017.feb., 2016.
1598
1599 Knutsen, S.-M. and Larsen,K.I.,: The late Mesozoic and Cenozoic evolution of the
1600 Sørvestsnaget Basin: A tectonostratigraphic mirror for regional events along the
1601 Southwestern Barents Sea Margin? Marine and Petroleum Geology, 14(1), 27-54,
1602 1997.
1603
1604 Kristensen, T.B., Rotevatn, A., Marvik, M., Henstra, G.A., Gawthorpe, R.L. and
1605 Ravnås, R.: Structural evolution of sheared basin margins: the role of strain
1606 partitioning. Sørvestsnaget Basin, Norwegian Barents Sea, Basin Research, 2017), 1-
1607 23, doi:10.1111/bre.12235, 2017.
1608
1609 Le Calvez, J-H. and Vendeville, : Experimental designs to mode along strike-slip fault
1610 interaction. *in*: Scellart, W.P. & Passcheir, C. (eds.). Analogue Modeling of large-scale
1611 Tectonic Processes, Journal of Virtual Explorer, 7, 7-23, 2002.
1612
1613 Leever, K.A., Gabrielsen, R.H., Sokoutis, D. and Willingshofer, E.: The effect of
1614 convergence angle on the kinematic evolution of strain partitioning in transpressional
1615 brittle wedges: insight from analog modeling and high resolution digital image analysis.
1616 Tectonics, 30, TC2013, 1-25, doi: 10.1029/2009TC002649, 2011a.
1617
1618 Leever, K.A., Gabrielsen, R.H., Faleide, J.I. and Braathen, A.: A transpressional origin
1619 for the West Spitsbergen Fold and Thrust Belt - insight from analog modeling.
1620 Tectonics, 30, TC2014, 1- 24, doi: 10.1029/2010TC002753, 2011b.
1621
1622 Libak, A., Mjelde, R., Keers, H., Faleide, J.I. and Murai,Y.: An intergrated geophysical
1623 study of Vestbakken Volcanic Province, western Barents Sea continental margin, and
1624 adjacent oceanic crust, Marine Geophysical Research, 33(2), 187-207, 2012.
1625
1626 Lorenzo. J.M.: Sheared continental margins: an overview, Geo-Marine Letters, 17(1),
1627 1-3, 1997

1628 Lowell, J.D., 1972: Spitsbergen Tertiary orogenic belt and the Spitsbergen fracture
1629 zone, Geol. Soc. Am. Bull., 83, 3091–3102, doi:10.1130/0016-
1630 7606(1972)83[3091:STOBAT]2.0.CO;2, 1972.

1631 Lundin, E.R. and Doré, A.G.: A tectonic model for the Norwegian passive margin with
1632 implications for the NE Atlantic.: Early Cretaceous to break-up. Journal of the
1633 Geological Society London, 154, 545-550, 1997.
1634

1635 Lundin, E.R., Doré, A.G., Rønning, K. and Kyrkjebø. R.: Repeated inversion in the
1636 Late Cretaceous-Cenozoic northern Vøring Basin, offshore Norway, Petroleum
1637 Geoscience, 19(4), 329-341, 2013.
1638
1639 Luth, S., Willingshofer, E., Sokoutis, D. and Cloetingh, S.: analogue modelling of
1640 continental collision: Influence of plate coupling on manle lithosphere subduction,
1641 crustal deformation and surface topography, Tectonophysics, 4184, 87-102, doi:
1642 10.1016/j.tecto2009.08.043, 2010.

1643 Maher, H. D., Jr., Bergh,S., Braathen, A. and Ohta, Y.: Svartfjella, Eidembukta, and
1644 Daudmannsodden lineament: Tertiary orogen-parallel motion in the crystalline
1645 hinterland of Spitsbergen's fold-thrust belt, Tectonics, 16(1), 88–106,
1646 doi:10.1029/96TC02616, 1997.

1647 Mandl, G., de Jong, L.N.J. and Maltha, A.: Shear zones in granular material. Rock
1648 Mechanics, 9, 95–144, 1977.
1649
1650 Manduit, T. and Dauteuil, O.: Small scale modeling of oceanic transform zones, Journal
1651 of Geophysical Research, 101(B9), 20195-20209, 1996.
1652
1653 Mann, P.: Global catalogue, classification and tectonic origins o frestraining and
1654 releasing bends on active and ancient strike-slip fault systems. *in*: Cunningham, W.D.
1655 and Mann,P. (eds.), 2007: Tectonics of Strike-Slip Restraining and Releasing Bends,
1656 Geological Society London Special Publication, 290, 13-142, 2007.
1657
1658 Mann, P., Hempton, M.R., Bradley, D.C. and Burke,K.: Development of pull-apart
1659 basins. Journal of Geology, 91(5), 529-554, 1983.
1660
1661 Mascle, J. & Blarez, E.: Evidence for transform margin evolution from the Ivory Coast
1662 Ghana continental margin, Nature, 326, 378-381, 1987.
1663
1664 McClay. K.R., 1990: Extensional fault systems in sedimentary basins. A review of
1665 analogue model studies, Marine and Petroleum Geology, 7, 206-233, 1990.
1666
1667 Mitra, S.: Geometry and kinematic evolution of inversion structures. American
1668 Assiciation of Petroleum Geologists Bulletin, 77, 1159-1191, 1993.
1669
1670 Mitra, S. and Paul, D.: Structural geology and evolution of releasing and constratrining
1671 bends: Insights from laser-scanned experimental models, American Association of
1672 Petroleum Geologists Bulletin, 95(7), 1147-1180, 2011.
1673
1674 Morgenstern, N.R. and Tchalenko, J.S.: Microscopic structures in kaolin subjected to
1675 direct shear, Géotechnique, 17, 309-328, 1967.
1676
1677 Mosar, J., Torsvik, T.H. & the BAT Team: Opening of the Norwegian and Greenland
1678 Seas: Plate tectonics in mid Norway since the late Permian. in: E.Eide (ed.): BATLAS.
1679 Mid Norwegian plate reconstruction atlas with global and Atlantic perspectives.
1680 Geological Survey of Norway, 48-59, 2002.
1681
1682 Mouslopoulou, V., Nicol, A., Little, T.A. and Walsh,J.J.: Terminations of large-strike-

slip faults: an alternative model from New Zealand, in: Cunningham, W.D. and Mann, P. (eds.): Tectonics of Strike-Slip Restraining and Releasing Bends, Geological Society London Special Publication, 290, 387- 415, 2007.

Mouslopoulou, V., Nicol, A., Walsh, J.J., Beetham, D. and Stagpoole, V.: Quaternary temporal stability of a regional strike-slip and rift fault interaction. Journal of Structural Geology, 30, 451-463, 2008.

Myhre, A.M. and Eldholm, O.: The western Svalbard margin (74-80˚N). Marine and Petroleum Geology, 5, 134-156, 1988.

Myhre, A.M., Eldholm, O. and Sundvor, E.: The margin between Senja and Spitsbergen Fracture Zones: Implications from plate tectonics. Tectonophysics, 89, 33-50, 1982.

Naylor, M.A., Mandl, G and Sijpestijn, C.H.K.: Fault geometries in basement-induced wrench faulting under different initial stress states. Journal of Structural Geology, 8, 737-752, 1986.

Nemcok, M., Rybár, S., Sinha, S.T., Hermeston, S.A. and Ledvényioviá. L.: Transform margins: development, controls and petroeum systems – an introduction. in: Nemcok, M., Rybár, S., Sinha, S.T., Hermeston, S.A. and Ledvényiová, L. (eds.): Transform Margins,: Development, Control and Petroleum Systems, Geological Society London, Special Publication, 431, 1-38, 2016.

Odonne, F. and Vialon, P.: Analogue models of folds above a wrench fault, Tectonophysics, 990,31-46, 1983

Pace, P. and Calamita, F.: Push-up inversion structures v. fault-bend reactivation anticlines along oblique thrust ramps: examples from the Apennines fold-and-thrust-belt, Italy, Journal Geological Society London, 171, 227-238, 2014.

Pascal, C. and Gabrielsen, R.H.: Numerical modelling of Cenozoic stress patterns in the mid Norwegian Margin and the northern North Sea. Tectonics, 20(4), 585-599, 2001.

Pascal, C., Roberts, D. and Gabrielsen, R.H.: Quantification of neotectonic stress orientations and magnitudes from field observations in Finnmark, northern Norway. Journal of Structural Geology, 27, 859-870, 2005.

Peacock, D.C.P., Nixon, C.W., Rotevatn, A., Sanderson, D.J. and Zuluaga, L.F.: Glossary of fault and other fracture networks, Journal of Structural Geology, 92, 12-29, doi: 10.1016/j.jgs2016.09.008, 2016.

Perez-Garcia, C., Safranova, P.A., Mienert, J., Berndt, C. and Andreassen, K.: Extensional rise and fall of a salt diapir in the Sørvestsnaget Basin, SW Barents Sea. Marine and Petroleum Geology, 46, 129-134, 2013.

Planke, S., Alvestad, E. and Eldholm, O.: Seismic characteristics of basaltic extrusive and intrusive rocks: The Leading Edge, 18(3), 342-348. https://doi-org.ezproxy.uio.no/10.1190/1.1438289, 1999.

Ramberg, H.: Gravity, deformation and the Earth's crust, Academic Press, New York, 214pp, 1967.

Ramberg, H.: Gravity, deformation and the Earth's crust, 2nd edition. Academic Press, New York 452pp, 1981

Ramsay, J.G. and Huber, M.I., 1987: The techniques of modern structural geology. Vol. 2: Folds and fractures. Academic Press, London, 309-700, 1987.

Reemst, P., Cloetingh, S. and Fanavoll,S.: Tectonostratigraphic modelling of Cenozoic uplift and erosion in the south-western Barents Sea. Marine and Petroleum Geology, 11, 478-490, 1994.

Richard, P.D., Ballard, B., Colletta, B and Cobbold, P.R.: Naissance et evolution de failles au dessus d'un décrochement de socle: Modeléisation experimental et tomographie, C. R. Acad.Sci. Paris, 308,9, 2111-2118, 1989.

Richard, P.D. and Cobbold, P.R.: Structures et fleur positives et décrochements crustaux: mdélisation analogiuque et interpretation mechanique, C.R.Acad.Sci.Paris, 308, 553-560, 1989.

Richard, P. and Krantz, R.W.: Experiments on fault reactivation in strike-slip mode, Tectonophysics, 188, 117-131, 1991.

Richard, P., Mocquet, B. and Cobbold, P.R., 1991: Experiments on simultaneous faulting and folding above a basement wrench fault, Tectonophysics, 188, 133-141. 1991.

Riedel,W.: Zur Mechanik geologischer Brucherscheinungen. Centralblatt für Mineralogie, Geologie und Palentologie, 1929B, 354-368, 1929.

Riis, F., Vollset, J. & Sand, M.: Tectonic development of the western margin of the Barents Sea and adjacent areas. in: M.T.Halbouty (ed.): Future petroleum provinces of the World. American Association of Petroleum Geologists Memoir, 40, 661-667, 1986.

Roberts, D.G., : Basin inversion in and around the British Isles, in: M.A.Cooper & G.D.Williams (eds.): Inversion Tectonics. Geological Society of London Special Publication, 44, 131-150, 1989.

Ryseth, A., Augustson, J.H., Charnock, M., Haugsrud, O., Knutsen., S.-M-, Midbøe, P.S., Opsal, J.G. and Sundsbø,G.: Cenozoic stratigraphy and evolution of the Sørvestsnaget Basin, southwestern Barents Sea. Norwegian Journal of Geology, 83, 107-130, 2003.

Saunders, A.D., Fitton, J.G., Kerr, A.C., Norry, M.J., and Kent, R.W.: The North Atlantic Igneous Province: Geophysical Monograph 100, American Geophysical Union, 45–93, 1997.

Scheurs, G.: Experiments on strike-slip faulting and block rotation, Geology, 22,567-

570, 1990.

Schreurs, G.: Fault development and interaction in distributed strike-slip shear zones: an experimental approach. *in:* Storti, F., Holdsworth, R.E. and Salvini, F. (eds): Intraplate Strike-slip Deformation Belts, Geological Society of London Special Publication, 210, 35-82., 2003.

Schreurs, G., and Colletta, B.. Analogue modelling of faulting in zones of continental transpression and transtension. *in:* Holdsworth, R.E., Strachan, R.A., Dewey, J.F. (eds.), Continental Transpressional and Transtensional Tectonics, Geological Society of London Special Publication, London, 135, 59–79, 1998.

Schreurs, G. and Colletta, B.: Analogue modelling of continental transpression and transtension. *in:* Scellart,W.P. & Passchier,C. (eds.): Analogue Modelling of Large-scale Tectonic Processes. Journal of the Virtual Explorer, 7, 103-114, 2003.

Seiler, C., Fletcher, J.M., Quigley, M.C., Gleadow, A.J and Kohn, B.P.: Neogene structural evolution of the Sierra San Felipe, Baja California: evidence of proto-gulf transtension in the Gulf Extensional Province? Tectonophysics, 488(1), 87-109, 2010.

Sibuet, J.C. and Mascle ,J.: Plate kinematic implications of Atlantic equatorial fracture zone trends. Journal of Geophysical Research, 85, 3401-3421, 1978.

Sims, D., Ferrill, D.A. and Stamatakos, J.A.: Role of a brittle décollement in the development of pull-apart basins: experimental results and natural examples. Journal of Structural Geology, 21, 533-554, 1999.

Sokoutis D.: Finite strain effects in experimental mullions. Journal of Structural Geology, 9, 233-249, 1987.

Stearns, D.W., 1978: Faulting and forced folding in the Rocky Mountains Foreland, Geological Society of America Memoir, 151, 1-38, 1978

Sylvester, A.G. (ed); 1985: Wrench Fault Tectonics, Selected papers reprinted from the AAPG Bulletin and other geological journals, American Association of Petroleum Geologists Reprint Series 28,3 74pp, 1985.

Sylvester, A.G.: Strike-slip faults. Geological Society of America Bulletin, 100, 1666-1703, 1988.

Taylor,B., Goodlife,A. and Martinez,F.: Intiation of transform faults at rifted continental margins, Comtes Rendu Geosciences, 341, 428-438, 2009.

Talwani, M. & Eldholm, O.: Evolution of the Norwegian-Greenland Sea. Geological Society of America Bulletin, 88, 969-999, 1977.

Tchalenko, J.S: Similarities between shear zones of different magnitudes. Geological Society of America Bulletin, 81, 1625-1640,1970

Tron, V. and Brun J-P.: Experiments on oblique rifting in brittle-ductile systems. Tectonophysics, 188(1/2), 71-84, 1991.

1829 Twiss, R.J. and Moores, E.M.: Structural Geology, 2nd Edition, W.H.Freeman & Co.,
1830 New York, 736pp, 2007.
1831
1832 Ueta, K., Tani ,K. and Kato,T.: Computerized X-ray tomography analysis of three-
1833 dimensional fault geometries in basement-induced wrench faulting, Engineering
1834 Geology, 56, 197-210, 2000
1835
1836 Uliana, M.A., Arteaga, M.E., Legarreta, L., Cerdan, J.J. and Peroni, G.O.: Inversion
1837 structures and hydrocarbon occurrence in Argentia. *in*: Buchanan,J.G. &
1838 Buchanan,P.G. (eds.): Basin Inversion, Geological Society London Special
1839 Publication, 88, 211-233, 1995
1840
1841 Vågnes,E.,1997: Uplift at thermo-mechanically coupled ocean-continent transforms:
1842 modeled at the Senja Fracture Zone, southwestern Barents Sea. Geo-Marine Letters,
1843 17, 100-109, 1997.

1844 Vågnes, E., Gabrielsen, R.H. and Haremo. P.: Late Cretaceous-Cenozoic intraplate
1845 contractional deformation at the Norwegian continental shelf: timing, magnitude and
1846 regional implications. Tectonophysics, 300, 29-46, 1998.

1847 Weijermars, R. and Schmeling, H.:. Scaling of Newtonian and non-Newtonian fluid
1848 dynamics without inertia for quantitative modelling of rock flow due to gravity
1849 (including the concept of rheological similarity. Physics of the Earth and Planetary
1850 Interiors, 43, 316–330, 1986.

1851 Wilcox, R.E., Harding, T.P. and Selly,D.R.: Basic wrench tectonics. American
1852 Association of Petroleum Geologists Bulletin, 57, 74-69, 1973
1853
1854 Williams, G.D., Powell, C.M., and Cooper, M.A.: Geometry and kinematics of
1855 inversion tectonics. in: M.A.Cooper & G.D.Williams (eds.): Inversion Tectonics.
1856 Geological Society of London Special Publication, 44, 3-16, 1989.
1857
1858 Willingshofer, E., Sokoutis, D. and Burg, J.-P.: Lithosprer-scale analogue modelling of
1859 collsion zones with a pre-existing weak zone, *in*: Gapais,D., Brun.,J.P.& Cobbold,P.R.
1860 (eds.): DeformatiomMechanisms, Rhology and Tectonics: from Minerals to the
1861 Litohsphere, Geological Society London Special Publication,43, 277-294, 2005.
1862
1863 Willingshofer, E., Sokoutis, D., Beekman ,F. Schönebeck, F., Warsitzka, J.-M., Michael,
1864 M. and Rosenau, M.: Ring shear test data of feldspar sand and quartz sand used in the
1865 Tectonic Laboratory (TecLab) at Utrecht University for experimental Earth Science
1866 applications. V. 1. GFZ Data Service. https://doi.org/10.5880/fidgeo.2018.072, 2018.
1867
1868 Woodcock, N.H. and Fisher, M.,1986: Strike-slip duplexes. Journal of Structural
1869 Geology, 8(7), 725-735, 1986.
1870
1871 Woodcock, N.H. and Schubert, C.: Continental strike-slip tectonics. in: P.L.Hancock
1872 (ed.): Continental Deformation (Pergamon Press), 251-263, 1994.
1873

Yamada, Y. and McClay, K.R.: Analog modeling of inversion thrust structures, experiments of 3D inversion structures above listric fault systems, in: McClay,K.R. (ed.): Thrust Tectonics and Petroleum Systems, American Association of Petroleum Geologists Memoir, 82, 276-302, 2004.